

News-Driven Uncertainty Fluctuations

Dongho Song

Boston College

Jenny Tang*

Federal Reserve Bank of Boston

This Version: January 3, 2018

Abstract

We embed a news shock, a noisy indicator of the future state, in a two-state Markov-switching growth model. Our framework, combined with parameter learning, features rich history-dependent uncertainty dynamics. We show that bad news that arrives during a prolonged economic boom can trigger a “Minsky moment”—a sudden collapse in asset values. The effect is greatly amplified with preference for early resolution of uncertainty. We leverage survey recession probability forecasts to solve a sequential learning problem and estimate the full posterior distribution of model primitives. We identify historical periods in which uncertainty and risk premia were elevated due to news.

Key words: Bayesian learning, discrete environment, Minsky moment, news shocks, recursive utility, risk premium, survey forecasts, uncertainty.

JEL codes: C11, G12, E32, E37.

*Correspondence: Department of Economics, Boston College, 140 Commonwealth Avenue, Maloney Hall 382, Chestnut Hill, MA 02467. Email: dongho.song@bc.edu. Research Department, Federal Reserve Bank of Boston, 600 Atlantic Avenue, T-9 Boston, MA 02210. Email: jenny.tang@bos.frb.org. The views expressed in this paper are those of the authors and do not necessarily represent the views of the Federal Reserve Bank of Boston or the Federal Reserve System. We thank Andre Kurmann, Minchul Shin, Jonathan Wright, and the seminar and conference participants at Boston College, the 2017 Society for Economic Measurement Conference, the 2017 NBER Time-Series Conference at Northwestern University, and the 2017 NBER DSGE Meeting at the Federal Reserve Bank of Philadelphia for helpful comments.

1 Introduction

Important news may come in the form of regular releases of macroeconomic data, policy announcements, or less frequent events (e.g., election results, terror attacks, crisis, etc). The literature has developed with an overwhelming focus on identifying economically important news.¹ However, there have been relatively fewer attempts to understanding the channels through which news influences subjective beliefs of economic agents, especially higher moments of beliefs.² Several important questions are left unanswered in the literature. For example, does more information about the future always reduce subjective uncertainty? Should news that contradicts existing beliefs about the future state raise uncertainty? Should we expect a differential effect on subjective uncertainty when receiving good news in a good state compared to receiving good news in a bad state? Would bad news have a different effect depending on when it arrives? To what extent would the behavior of quantities such as subjective uncertainty change when news is believed to be of greater informative value?

In this paper, we aim to incorporate news into an otherwise standard model in order to answer these questions. Within a parsimonious two-state Markov-switching growth model, we introduce an agent who receives news in every period that reveals the next period's state with some error. We consider cases where the agent can rationally learn model parameters, including state transition probabilities or the accuracy of this news, using Bayes' rule as new data arrive. This model produces two novel properties of the influence of news on subjective uncertainty. First, we show that when news contradicts prior beliefs, uncertainty can increase as the agent's posterior beliefs get corrected to a more uniform distribution. For empirically plausible parameter values, the rise in uncertainty is more apparent when news is believed to be more accurate. This is in contrast to a Gaussian environment in which news always reduces uncertainty.³ The

¹There is a growing literature that attempts to identify economically important news and their impact on financial markets (e.g., Boyd, Hu, and Jagannathan (2005), Gurkaynak, Sack, and Swanson (2005), Andersen, Bollerslev, Diebold, and Vega (2007), Faust and Wright (2007), Savor and Wilson (2013), Lucca and Moench (2015), Tang (2017), among others).

²The existing literature studying the effect of news shocks (see Beaudry and Portier (2006), Jaimovich and Rebelo (2009), Barsky and Sims (2011), Schmitt-Grohe and Uribe (2012), Kurmann and Otrok (2013), Beaudry and Portier (2014), and Malkhozov and Tamoni (2015)) focuses mainly on the transmission of these shocks to asset prices or the economy through their effects on agents' mean beliefs about future outcomes.

³Veronesi (1999) shows a similar relationship between dividend growth realizations and uncertainty in a model without news where agents must learn about a hidden dividend growth state. See the literature review below for a more extensive discussion.

discrete-state environment thus allows news to drive large fluctuations in subjective uncertainty even without stochastic volatility.

In addition to this above result, we show that as the agent learns either the accuracy of news or the persistence of states, the effect of news on uncertainty is altered, thus giving rise to history-dependent behavior in uncertainty fluctuations. As a result, parameter learning can greatly amplify the response of uncertainty to news. To illustrate the intuition, suppose that the economy stays in a good state with the agents receiving good news, which is correct ex-post, for an extended period of time. In this setting, the agent successively increases her estimate of the accuracy of news and subjective uncertainty gradually falls as more good news arrives. When bad news arrives against this backdrop, the agent, now believing that news is very accurate, sharply adjusts beliefs toward a more uniform posterior distribution which results in an upward jump in subjective uncertainty. In this example, the jump in uncertainty upon receiving bad news will be larger for longer runs of consecutive “good state, good news” realizations prior to the arrival of bad news. In general, parameter learning introduces additional state variables to the model that summarize information from past states and alters the effect of news on agent’s beliefs.

In light of these findings, we examine the extent to which news-driven uncertainty fluctuations can generate variation in asset prices. We consider an agent that has preference for early resolution of uncertainty in an endowment economy with a two-state Markov-switching growth process. We first isolate the role of news without parameter learning. It is interesting to highlight the implications for asset prices when beliefs about state persistence and news accuracy are identical and close to one. In this setting, switching states, which occur when news contradicts existing beliefs about future state, are ones in which the agent thinks that there is equal chance of entering a nearly permanent good or bad state in the next period. Note that this cannot occur in a standard discrete-state Markov-switching model without news shocks since probabilities of future state realizations are tightly linked to state persistence in that setting. News shocks break this link and thus create the potential for these episodes of extreme uncertainty and, as a result, highly elevated risk premia. Even for very moderate values of risk aversion and the intertemporal elasticity of substitution, both set to 1.5, the implied risk premium on a consumption claim can reach up to 5% in these switching states, roughly 160 times larger than the counterfactual risk premium under log utility. In this highly uncertain state, demand for the risky consumption claim is very low and the

agent requires a very high expected excess return on this asset in order to equilibrate shorting demand with the asset’s zero net supply.

We then consider the theoretical implications of parameter learning in our model with news shocks. We first illustrate qualitative results using the anticipated utility approach to price assets.⁴ We highlight the case of high prior means for the state persistence and news accuracy parameters in an experiment similar to the one mentioned above for forecast uncertainty in which bad news arrives after a prolonged economic boom. The excessive optimism built by the agent with preference for early resolution of uncertainty, i.e., the increase in her posterior beliefs of staying in the good state, leads to a “Minsky moment” once the agent suddenly receives news that the future may not be as bright as expected.⁵ The size of the risk premium is twice larger than the one that would have been obtained without parameter learning.

Next, we take our model to the data. To obtain estimates of news parameters and realizations, we leverage a forward-looking variable that summarizes agents’ information about the future state. Since agents in our model generate discrete belief distributions over future states based on both current fundamentals and potentially noisy news about the future state, we map their believed bad state probabilities to recession probability forecasts from the Survey of Professional Forecasters. We make an important technical innovation that allows us to use this variable to recover parameter estimates and filtered states, including news realizations. Specifically, we develop a novel filtering technique that uses both actual GDP growth and recession probability forecasts in the estimation. This technique can be interpreted as a sequential learning problem of an econometrician who observes only these two variables. We solve this problem and sample from the joint posterior of model parameters and states by augmenting the filtering technique with the particle learning algorithm developed by Carvalho, Johannes, Lopes, and Polson (2010). Using data starting in 1969, we obtain the full posterior distribution of model primitives, including the filtered distribution of news, which characterizes the econometrician’s full learning problem.

⁴Johannes, Lochstoer, and Mou (2016) study parameter learning using an anticipated utility approach in a model with long-run risks but without news shocks and show that revisions in beliefs about consumption dynamics are quite volatile and pricing assets using these beliefs improves the model’s ability to fit moments as well as the historical path of equity prices. Collin-Dufresne, Johannes, and Lochstoer (2016) shows that allowing fully rational pricing of parameter uncertainty further helps the model to match asset pricing facts. See also Bansal and Yaron (2004).

⁵The “Minsky moment,” which stems from the work of Hyman Minsky, originally implies a sudden collapse of markets and economies after a long period of growth, sparked by debt or currency pressures.

Our main empirical findings are threefold. First, we show that posterior beliefs vary significantly over time and, in particular, there is a pattern of higher forecast uncertainty driven by bad news during expansions relative to an estimation that does not allow for news shocks. In light of this property of our model, we expect news-driven uncertainty fluctuations to be important for generating sizable fluctuations in endogenous variables within growth regimes. Second, the estimated recession probability tightly identifies NBER recession dates. When only GDP growth is used in the estimation (without recession probability forecasts), the model’s filtered recession probabilities tend to be biased upward with bad states being less tightly identified. Third, we show that our model-implied probability of receiving bad news correlates strongly (around 0.6) with an index measuring the prevalence of bad news from the University of Michigan’s Survey of Consumers. This serves as an external validation check. We also find that our news measure strongly negatively predicts one-step ahead GDP growth after controlling for other factors as implied by the model.

Lastly, to assess our model’s quantitative implications for asset prices, we incorporate our empirical findings into an asset pricing model in which the agent must learn the transition probabilities of growth states and this parameter uncertainty is rationally priced. To do so, we extend the policy function iteration method used in Collin-Dufresne, Johannes, and Lochstoer (2016) to accommodate a news shock and obtain a fully nonlinear solution of the model. Adding news to this model changes both the risks coming from parameter uncertainty, by speeding up learning about transition probabilities, as well as the risks coming from regime uncertainty, through the mechanisms described above.

Using our estimated model parameters and filtered regime probabilities, we find that news shocks produce modest increases in both risk-free rates and equity risk premia while having a substantially larger impact on their volatility. This increase in volatility is particularly pronounced during economic expansions. Including news shocks in the model increases the standard deviation of equity premia within high growth states by over 6.7 times. News shocks greatly improve the model’s ability to match the conditional and unconditional volatilities of risk-free rates and equity premia in the data.

This increased volatility is evident in the time series of equity premia produced by our estimates. Furthermore, our estimates indicate that bad news arriving prior to recessions often lead equity premia to begin rising several quarters prior to the onset of recessions. Bad news in our model can also generate large spikes in equity premia even when contemporaneous GDP growth remains high, such as during the Black Monday

crash. This effect is amplified by the increase in subjective uncertainty when bad news contradicts the concurrent growth state. Equity premia generated by an identically calibrated model without news shocks do not have these features.

Literature Review. This paper is at the intersection of several literatures. First, it is related to papers that study news shocks theoretically and empirically in the context of asset pricing (such as Beaudry and Portier (2006), Kurmann and Otrok (2013), and Malkhozov and Tamoni (2015)) as well as business cycles (such as Jaimovich and Rebelo (2009), Barsky and Sims (2011), Schmitt-Grohe and Uribe (2012), and the works surveyed in Beaudry and Portier (2014)). Unlike most of this existing work which focuses on the effect of news on mean forecasts of future economy activity, we focus on the additional effects that news shocks have on uncertainty. We also consider how news shocks affect parameter learning and their joint effects on uncertainty.

Our paper is also very closely related to studies that examine the sources of uncertainty fluctuations. In particular, Kozeniauskas, Orlik, and Veldkamp (2016) also study uncertainty in a model that features parameter learning, but without news shocks. Stochastic volatility and disaster risks are crucial for generating uncertainty fluctuations in their environment. In contrast, we show that news shocks can generate uncertainty fluctuations even when the true data-generating process does not have stochastic volatility. The recent work by Berger, Dew-Becker, and Giglio (2017) uses an estimated VAR to separate exogenous shocks to expected volatility from movements in realized volatility. In contrast, our setting does not allow for an exogenous shock to uncertainty. Instead, uncertainty in our model fluctuates with realizations of actual economic data and news shocks about future regimes.

Our finding of a state-dependent relationship between news and uncertainty is related to Veronesi (1999) which also models asset prices in a setting with non-Gaussian random variables. That paper obtains a similar relationship between observations of a dividend process and uncertainty in a model without news shocks where agents must learn about a hidden Markov state that determines dividend growth. In contrast, we find this state-dependent relationship in a setting in which the agent knows the current state but receives noisy news about the future state. We further explore the potential for rich history-dependent behavior of uncertainty when the agent must also learn particular parameters of the model. Additionally, we take the model to the data and empirically identify historical episodes in which uncertainty about future GDP growth was elevated due to news.

On the methodological side, Bianchi (2016) and Bianchi and Melosi (2016) provide analytical characterizations of uncertainty in Markov-switching models under both perfect information and settings where the agent must infer states and unknown parameter values through Bayesian learning, respectively. Our paper differs from these by focusing on the effect of news about the future (rather than signals about the current state) on uncertainty. We additionally provide an empirical estimation of the model as well as an analysis of the asset pricing implications of allowing for news.

Our empirical exercise is closely related to Milani and Rajrhandari (2012), Hirose and Kurozumi (2012), and Miyamoto and Nguyen (2015), which all incorporate forecast data into the estimation of news shocks. Nonetheless, there remain two key differences. First, we develop new econometric methods that allow us to include recession probability forecasts in the estimation while these papers focus on only mean forecasts. Furthermore, these studies estimate DSGE models with shocks to news about particular structural shocks (e.g., TFP, demand, monetary policy, etc.). In contrast, we remain agnostic about the types of structural shocks that news may pertain to and instead estimate a latent news variable summarizing all information that is embedded in the recession probability forecasts and is not already captured by the current GDP growth state.

In addition to the above-mentioned asset pricing papers that consider parameter learning, our asset pricing application is also related to work featuring models where agents can form beliefs from sources of data other than simply realized GDP growth rates. The works of Johannes, Lochstoer, and Mou (2016) and Constantinides and Ghosh (2016) allow agents to form beliefs by incorporating additional information from multiple sources of macroeconomic data—namely consumption, output, and/or labor market variables. However, in contrast to our paper, these studies model these additional variables as being informative only about the current state of the economy and not about future regimes. Furthermore, these papers do not use forecast data in their estimations while we do. The use of such forecast data allows us to be agnostic about the sources of additional information and instead capture a summary of information relevant for forecasting future output.

In Section 2, we first describe our model of real output growth and news shocks. Section 3 presents the estimation of these exogenous driving processes. Section 4 presents stock market moments implied by these estimated values and Section 5 concludes.

2 Modeling News

2.1 The environment

We begin with the following two-state Markov-switching model for real GDP growth:

$$\begin{aligned} y_t &= \mu_{S_t} + \sigma_{S_t} \epsilon_t, \quad \epsilon_t \sim N(0, 1), \\ \Pr(S_t = j | S_{t-1} = i) &= q_{ij} \quad \text{with} \quad \sum_j q_{ij} = 1. \end{aligned} \tag{1}$$

Here y_t represents the real GDP growth rates and S_t is a discrete Markov state variable that takes on two values $S_t \in \{1, 2\}$. We assume $\mu_1 > \mu_2$ without loss of generality.

We introduce news that provides information about next period's state,

$$n_t = S_{t+1}, \quad \text{w.p. } \chi, \quad 0.5 \leq \chi \leq 1, \tag{2}$$

which is available in discrete form.⁶ We assume that n_t can predict the future state with probability χ . The accuracy of the prediction increases with χ . The combination of two discrete Markov chains, one for the fundamental variable in (1) and the other for the news component in (2), results in the four-state Markov chain process. The model parameters are collected in

$$\theta = \{\mu_1, \mu_2, \sigma_1^2, \sigma_2^2, \chi, \sigma_z^2\}, \quad \Pi = \{q_{11}, q_{22}\}.$$

σ_z^2 parameterizes an error process that will be introduced in Section 3 when we estimate the model.

In terms of parameter learning, we will mainly focus on the case of learning about the transition probabilities, q_{11} and q_{22} , based on observing the true states and news realizations.⁷ The Bayesian updating problem is detailed in Appendix A.

⁶Note that the label switching problem arises for χ values smaller than 0.5. Therefore, we restrict to $0.5 \leq \chi \leq 1$.

⁷Our notation will reflect that real GDP growth is also in the information set of agents, but growth state and news realizations alone are sufficient for Bayesian learning about q_{11} and q_{22} .

2.2 News implications

State prediction and parameter learning accuracy. We demonstrate how the prediction of the future state and posterior beliefs about the transition probabilities are affected by the accuracy of news. For ease of illustration, we work with conditional distributions and assume a subset of model parameters and the history of states might be known at time t when relevant.

We consider two boundary values of $\chi \in \{0.5, 1\}$. We start from $\chi = 0.5$ in which news contain no information about the future state. Because it assigns equal probability to both states, the predictive distribution of the future state conditional on news is identical to the one without conditioning on news

$$p(S_{t+1} = 1|n_t, S^t, \Pi, \theta) = p(S_{t+1} = 1|S^t, \Pi, \theta).$$

Analogously, when agents must learn transition probabilities, we can deduce that news has no impact on the posterior mean of these parameters when $\chi = 0.5$

$$E(q_{ii}|n_t, y^t, S^t, \theta) = E(q_{ii}|y^t, S^t, \theta).$$

On the other hand, if news contains certain information about the future state, that is, $\chi = 1$, then knowledge about the current state no longer plays a role in predicting the future state. The state prediction becomes a degenerate distribution function

$$p(S_{t+1} = 1|n_t, S^t, \Pi, \theta) = p(S_{t+1} = 1|n_t, \theta) = \begin{cases} 1, & \text{if } n_t = 1 \\ 0, & \text{otherwise.} \end{cases}$$

Because the future state is known with certainty, the posterior mean of transition probabilities is identical to the one that would have been obtained in time $t + 1$ in the absence of news

$$E(q_{ii}|n_t, y^t, S^t, \theta) = E(q_{ii}|y^{t+1}, S^{t+1}, \theta).$$

The above examples show that news can lead to improvement in prediction and parameter learning accuracy. Detailed derivations are provided in Appendix A and B.

Forecast uncertainty. The above examples illustrate that news improves ex-post

forecast accuracy, but we now consider the impact of news on ex-ante forecast uncertainty. In this model, one measure of forecast uncertainty is the conditional variance of one-period-ahead output growth defined as

$$\begin{aligned} Var(y_{t+1}|y^t, S^t, n^t, \Pi, \theta) &= \int (y_{t+1} - y_{t+1|t})^2 p(y_{t+1}|y^t, S^t, n^t, \Pi, \theta) dy_{t+1} \\ &= \underbrace{\sigma_1^2 + (q_{3i}^B + q_{4i}^B)(\sigma_2^2 - \sigma_1^2)}_{\text{due to second moment}} + \underbrace{(q_{1i}^B + q_{2i}^B)(q_{3i}^B + q_{4i}^B)(\mu_1 - \mu_2)^2}_{\text{due to first moment}} \end{aligned} \quad (3)$$

where $y_{t+1|t} = \int y_{t+1} p(y_{t+1}|y^t, S^t, n^t, \Pi, \theta) dy_{t+1}$ and $\sum_{j=1}^4 q_{ji}^B = 1$. q_{ji}^B are transition probabilities of an expanded state space that encompasses both the realizations of S_t and n_t . We refer the reader to expression (A-15) in the Appendix for the relationship between q_{ji} , χ , and q_{ji}^B . Forecast uncertainty (3) is comprised of two components: The first component captures uncertainty with respect to innovation variances and the second component arises from uncertainty about mean values. This is due to our discrete-state environment.

We now explain the effect of news on the transition probabilities q_{ji}^B by which uncertainty is determined. For ease of illustration, we assume that persistence of each regime is identical $q = q_{11} = q_{22}$ and use $\mu_1 = 0.84, \mu_2 = -0.22, \sigma_1^2 = 0.47, \sigma_2^2 = 0.56$.⁸ Figure 1 provides the value of forecast uncertainty as a function of $\chi \in [0.5, 1)$ for different values of $q \in [0.5, 1)$. We are only considering moderately persistent q values and excluding the end points ($q = 1, \chi = 1$) which would remove all state uncertainty. Note that by considering only $q \geq 0.5$, the most likely outcome for next period's state is always the current state when news is not part of the information set.

Panel (A) of Figure 1 isolates the usual stochastic volatility component of forecast uncertainty. As the accuracy of news increases, forecast uncertainty converges to the variance of the state indicated by the news realization. What is interesting to observe is panel (B) which isolates the part of uncertainty arising from different mean values (the final term in (3)). Note that this panel also illustrates the large fluctuations in uncertainty that can arise due to news in a setting without stochastic volatility. If news suggests that the current regime will persist next period, then forecast uncertainty monotonically decreases as χ increases, i.e., the first and fourth column. On the contrary, if news contradicts the implication of the current state alone and suggests switching into a different state, then forecast uncertainty increases in χ for $\forall \chi \leq q$ and

⁸These are the end-of-sample posterior median estimates presented in Section 3.

decreases in χ for $\forall \chi > q$. The intuition behind this result is that, with $q \in [0.5, 1)$, the current state is more likely to persist than not. News that suggests a switch in the state will shift the posterior distribution of next period’s state to a more uniform one where weight is placed more equally on the two possible realizations. Note that in order for this to occur, the news must be moderately informative. Completely uninformative news will not alter beliefs while perfectly informative news will shift beliefs to the limit where a switch will occur with certainty.

Panel (C) shows the forecast uncertainty when both channels are at play. It is important to note that the patterns are qualitatively similar to those shown in panel (B). The key takeaway is that, in contrast to standard Gaussian setups where more information always lowers uncertainty, our discrete-state environment allows moderately informative news to increase forecast uncertainty when it contradicts existing beliefs.

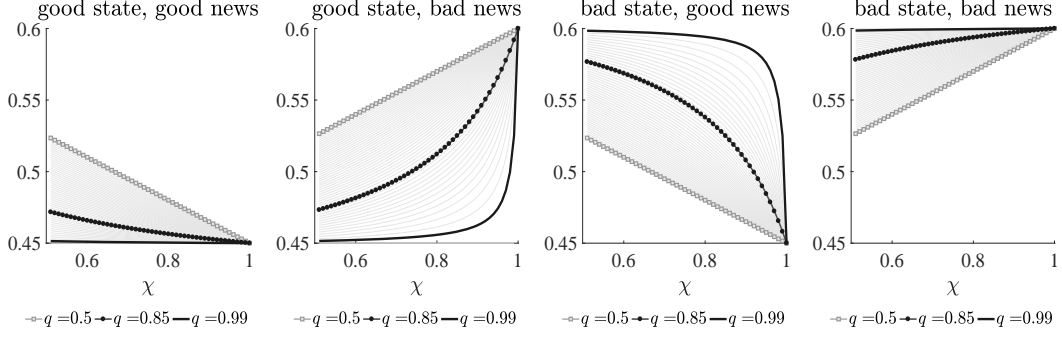
Having shown the role of news in forecast uncertainty, we discuss how parameter learning, in particular, learning about the accuracy of news and state persistence, can give rise to additional fluctuations in uncertainty and history-dependent behavior.⁹ Consider the following experiment in which for $t - 1$ consecutive periods, we are in good state and receive good news, but on t^{th} period we receive bad news while remaining in the good state. We calculate the corresponding forecast uncertainty (3) when the agent learns either state persistence or news accuracy and continue to use the assumption of $q = q_{11} = q_{22}$ along with $\mu_1 = 0.84, \mu_2 = -0.22, \sigma_1^2 = 0.47, \sigma_2^2 = 0.56$. For this exercise, learning begins with prior beliefs. We assume that the prior mean of the transition probability q is 0.8 and the prior for the news accuracy χ is 0.6. The length of the prior training sample is set to 8 periods. To focus on learning only about these parameters, we assume that the remaining parameters are known.

Figure 2 shows the case of $t \in \{4, 9\}$. We start with the case of learning the accuracy of news χ while beliefs about q never get updated. Panel (A) of Figure 2 plots the posterior evolution of χ and the corresponding forecast uncertainty using circles that darken as time progresses. As news is revealed to be correct for t consecutive periods (see “good state, good news”), beliefs about news accuracy continually improve. As a result of the improvement in news accuracy, forecast uncertainty gradually falls as more good news arrives. The circle corresponding to the arrival of bad news is plotted under

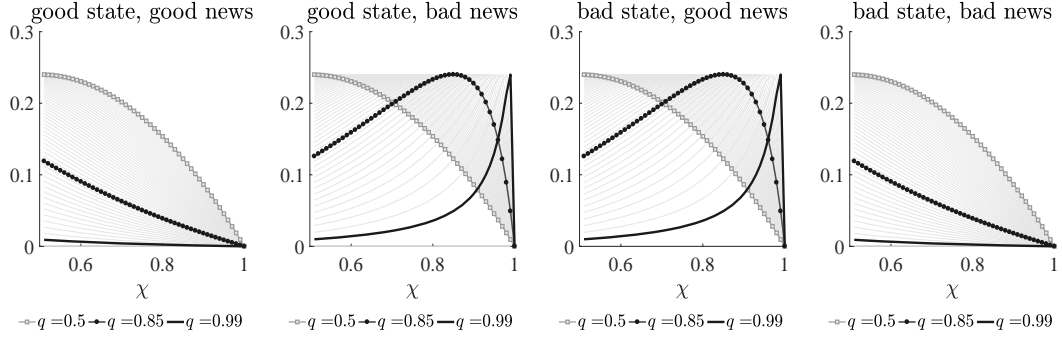
⁹The Bayesian learning process for news accuracy χ is analogous to those for state transition probabilities detailed in Appendix A with the main difference being that the posterior distribution of χ is updated in each period as past news is verified to be true or not.

Figure 1: The role of news in forecast uncertainty

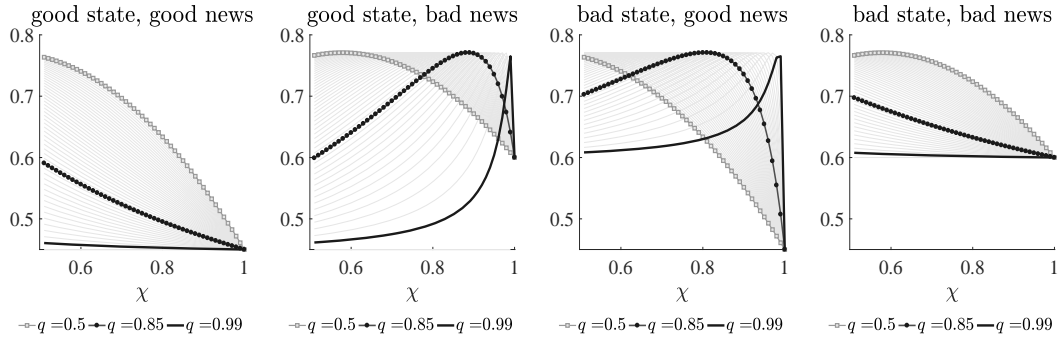
(A) Volatility channel



(B) Mean channel



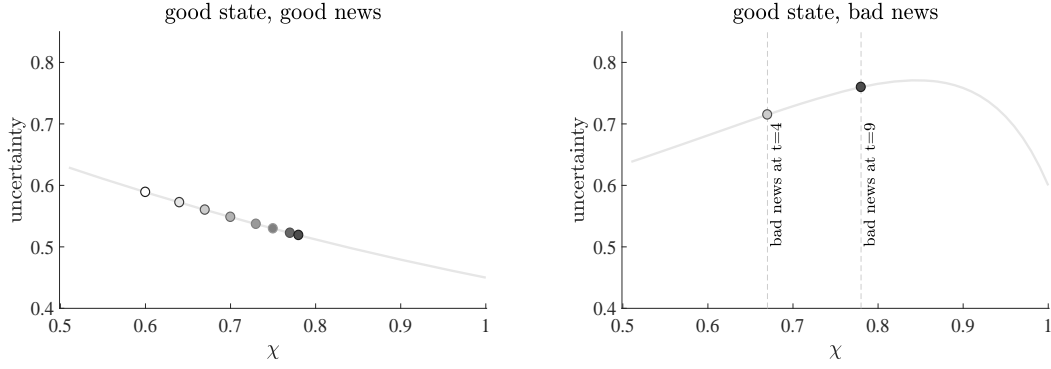
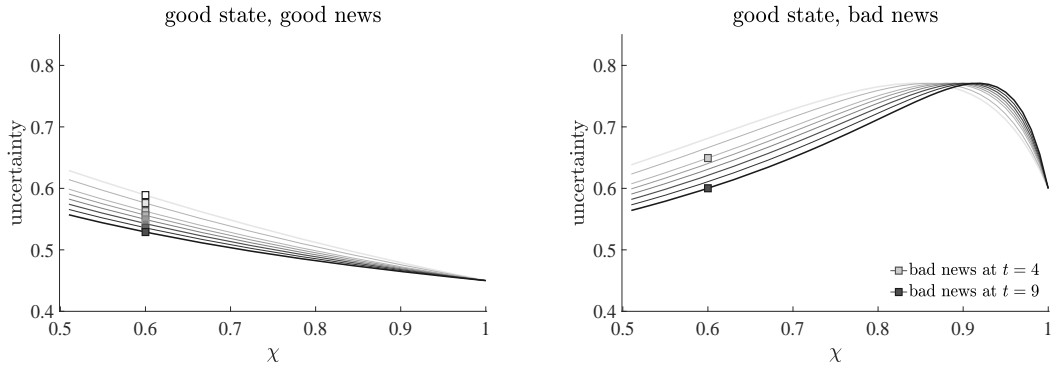
(C) Both channel



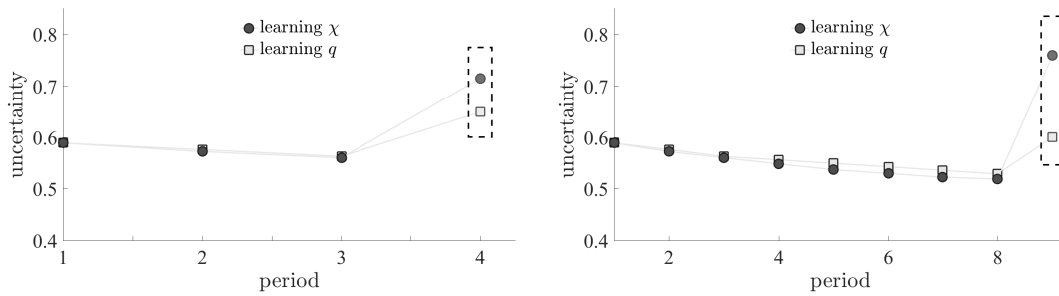
Notes: We assume $q = q_{11} = q_{22}$ and $\mu_1 = 0.84, \mu_2 = -0.22, \sigma_1^2 = 0.47, \sigma_2^2 = 0.56$. Squared-lines indicate when $q = 0.5$, circled-lines are when $q = 0.85$, and black-solid lines are when $q = 0.99$.

“good state, bad news.” Comparing the circles corresponding to $t = 4$ and $t = 9$ reveals that the longer the economy remains in “good state, good news” (the higher the t), the larger the jump in forecast uncertainty when bad news arrives. This is driven by two forces both of which stem from the fact that remaining in “good state, good news” for

Figure 2: The role of learning in forecast uncertainty

(A) Learning news accuracy χ (B) Learning state persistence q 

(C) Time-series of the implied uncertainty



Notes: For illustrative purpose, we assume $\mu_1 = 0.84, \mu_2 = -0.22, \sigma_1^2 = 0.47, \sigma_2^2 = 0.56$. The prior mean of the transition probability is 0.8. The prior for the news accuracy is 0.6. The length of the prior training sample is set to 8 periods. For $t-1$ consecutive periods, we are in good state and receive good news. On t^{th} period, we are still in good state, but receive bad news. We assume that bad news arrives at $t \in \{4, 9\}$. In the top and the middle panel, we use darker color to indicate the evolution of posterior beliefs. In the bottom panel, we use a dashed-box to indicate the implied uncertainty from bad news.

longer leads the agent to have a higher belief about news accuracy. This higher belief about χ has two implications. One is that, in the period just before the arrival of bad news, uncertainty is lower because the agent has more faith in the current good news realization. Secondly, the agent also believes the realization of bad news in the next period to be more accurate, thus shifting beliefs about S_{t+1} more in the direction of a uniform distribution. We plot the time series of the implied uncertainty for these two cases as circles (compare the first column with the second column) in panel (C).

Panel (B) provides the case of learning only state persistence q , but with beliefs about χ remaining at the prior of 0.6. Note that the first point in this case is the same as that in panel (A) because we still start from the prior $q = 0.8$. Thus, the line in panel (A) still appears in panel (B). However, we no longer remain on this line now that posterior beliefs about q improve over time. This results in further declines in forecast uncertainty up to (and including) time $t - 1$ as agents become more sure that they will remain in the good state. It is at time t when news contradicts the implication of the current state and suggests switching into the bad state that forecast uncertainty jumps up. However, both the level of uncertainty at time t and the jump from time $t - 1$ are lower than those under the case of learning news accuracy χ . We compare the time series of the implied uncertainty for these two cases as circles and squares in panel (C).

2.3 Embedding news in an asset pricing model

We have seen from the previous section that news shocks can generate significant variation in uncertainty, particularly when news contradicts existing beliefs, as well as rich history-dependent dynamics of uncertainty when combined with parameter learning. In light of these findings, we now examine the extent to which news-driven uncertainty fluctuations can generate variation in asset prices.

We consider an endowment economy with a representative agent that has Epstein and Zin (1989) preferences and maximizes lifetime utility,

$$V_t = \max_{C_t} \left[(1 - \beta) C_t^{\frac{1-\gamma}{\alpha}} + \beta (E_t V_{t+1}^{1-\gamma})^{\frac{1}{\alpha}} \right]^{\frac{\alpha}{1-\gamma}}, \quad (4)$$

subject to budget constraint $W_{t+1} = W_t R_{c,t+1} - C_{t+1}$, where C_t is consumption of the agent, W_t is wealth, $R_{c,t+1}$ is the return on wealth, β is the discount rate, γ is risk

aversion, ψ is the intertemporal elasticity of substitution (IES), and $\alpha = \frac{1-\gamma}{1-1/\psi}$. The stochastic discount factor (SDF) is

$$M_{t+1} = \beta^\alpha \left(\frac{C_{t+1}}{C_t} \right)^{-\gamma} \left(\frac{PC_{t+1} + 1}{PC_t} \right)^{\alpha-1} \quad (5)$$

where PC_t is the wealth-consumption ratio.

To precisely understand the role of news, we start from the case of log utility preference and move to the case of the recursive utility with preference for early resolution of uncertainty (i.e., $\gamma > 1/\psi$). The former is a special (limiting) case of the latter as $\gamma \rightarrow 1$ and $\psi \rightarrow 1$. We set $\beta = 0.994$ for both cases and use moderate values of $\gamma = 1.5$ and $\psi = 1.5$ for the latter one. Similar to the previous subsection, we assume that persistence of each regime is identical $q = q_{11} = q_{22}$ with values of $\mu_1 = 0.84, \mu_2 = -0.22, \sigma_1^2 = 0.47, \sigma_2^2 = 0.56$ for illustrative purposes. We also assume that all assets are in zero net supply so that $\Delta c_{t+1} = \Delta y_{t+1}$ and follows equation (1).

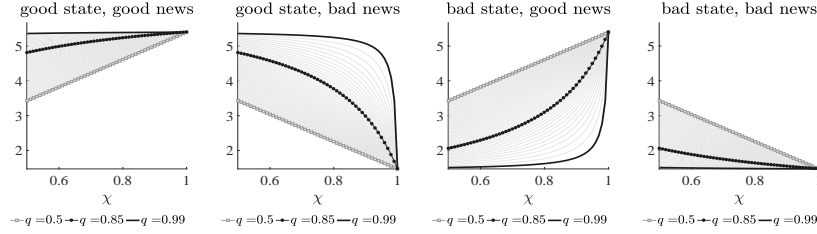
Figure 3 provides the corresponding values of the risk-free rate and the expected excess return (i.e., risk premium) on a consumption claim associated with each value of news accuracy χ and state persistence q . Panel (A) of Figure 3 shows the case of log utility preference where the implied SDF is a function only of consumption growth (see equation (5) when $\alpha = 1$). We find that the model-implied risk-free rate is procyclical and risk premium is countercyclical. In the limiting case of completely uninformative news, $\chi = 0.5$, there exist only two values of the risk-free rate (risk premium) with the higher (lower) value realized in the good state. As the news accuracy increases towards the case of perfectly informative news, $\chi = 1$, the risk-free rate (risk premium) converges to a case where there are again only two values, but ones that vary with news with the higher (lower) value realized under good news. The intuition from Figure 1 carries over to the current risk premium graph: news alters the expected path of consumption growth and can potentially give rise to higher risk premia when news suggests a switch in the state.

Panel (B) of Figure 3 provides the value of the risk-free rate and risk premium for the recursive utility case with preference for early resolution of uncertainty. For moderate values of q , we observe very similar patterns of the risk-free rate and risk premium to the ones from the log utility case. What is interesting to observe is the case of $q = 0.99$ and $\chi = 0.99$. In this case, the two switching news states are ones in which the agent thinks that there is equal chance of entering a nearly permanent good or bad state in the

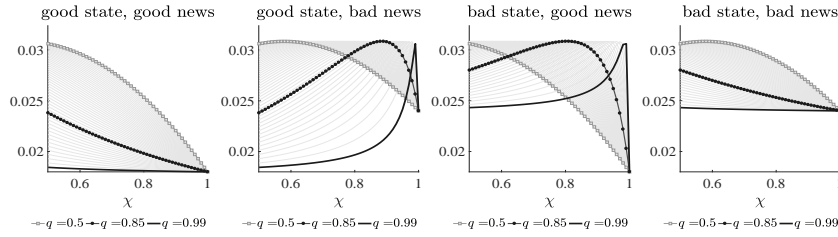
Figure 3: The role of news in asset prices

(A) Log utility

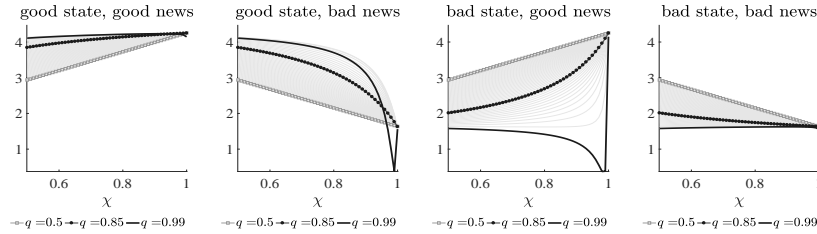
Risk-free rate



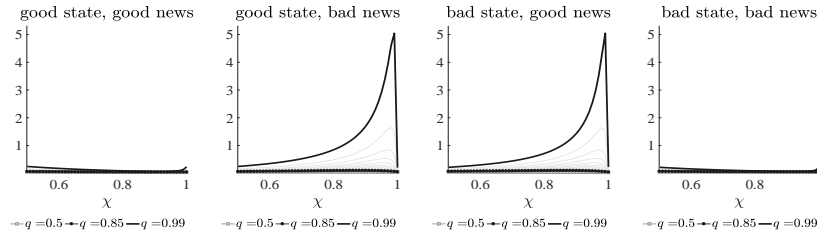
Expected excess return on consumption claim

(B) Preference for early resolution of uncertainty: $\gamma = 1.5, \psi = 1.5$

Risk-free rate



Expected excess return on consumption claim



Notes: We assume $q = q_{11} = q_{22}$ and $\mu_1 = 0.84, \mu_2 = -0.22, \sigma_1^2 = 0.47, \sigma_2^2 = 0.56$. Squared-lines indicate when $q = 0.5$, circled-lines are when $q = 0.85$, and black-solid lines are when $q = 0.99$. The numbers on y-axis are in annualized percent terms.

next period. We already learned from Figure 1 that the $q = \chi$ case maximizes the one-period ahead uncertainty. When it comes to asset prices, the effect is greatly amplified with a preference for early resolution of uncertainty when the underlying growth states are nearly permanent. Note that the implied risk premium can be up to 5% for the two switching news cases, which is roughly 160 times larger than the value from the log utility case, 0.03%. The extremely high uncertainty about very persistent states produces a strong desire for the agent to save in a safe asset. In equilibrium, returns on the risk-free asset must be lower to equilibrate the agent's desire to save with the zero net supply of risk-free assets. This is reflected in a sharply lower risk-free rate for the values of $q = 0.99$ and $\chi = 0.99$ compared to other parameter values. Similarly, demand for the risky consumption claim is very low in this environment and the agent requires a very high expected excess return on this asset in order to equilibrate shorting demand with the asset's zero net supply.

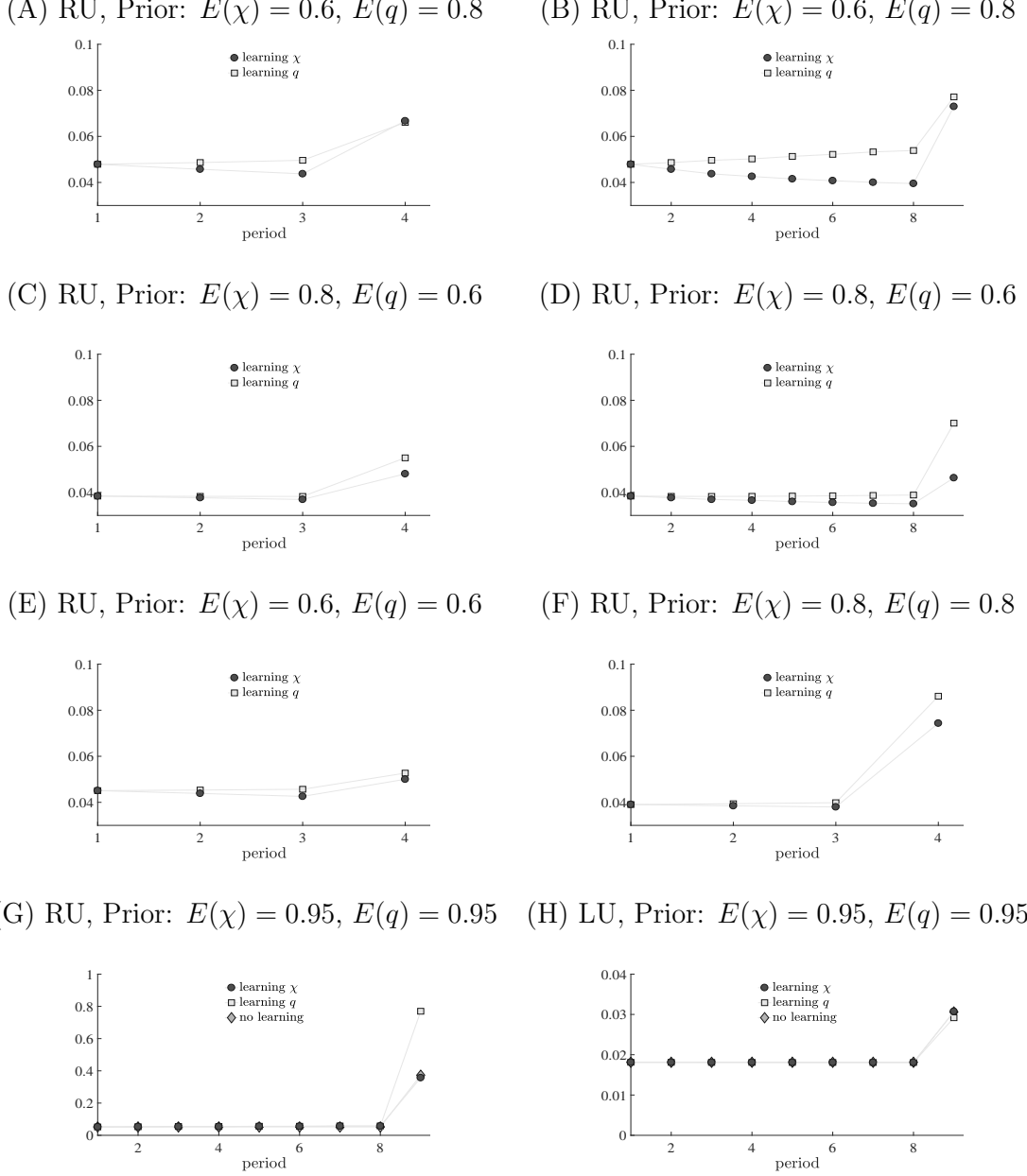
We now consider the implications of parameter learning in our model with news shocks. In a similar model without news shocks, Johannes, Lochstoer, and Mou (2016) are able to replicate several asset pricing moments.¹⁰ One key feature of Johannes, Lochstoer, and Mou (2016) is the generation of strongly countercyclical return volatility and a high equity premium in recessions through parameter learning. This is because the infrequent nature of recessions implies greater parameter updating when the economy visits that state. Thus, long-run shocks to parameter beliefs will be largest during recessions and this contributes to the high average equity premium in recessions. What is interesting is that, above and beyond the usual mechanics described in Johannes, Lochstoer, and Mou (2016), our model is able to generate large fluctuations in growth uncertainty within states through the addition of news shocks. On top of this, revisions in parameter beliefs in our model will further interact with news shocks in a way that can produce richer dynamics for asset prices.

For illustrative purposes in this subsection, we rely on the anticipated utility approach to price assets, as in Johannes, Lochstoer, and Mou (2016).¹¹ We later examine the case of fully rational pricing in which the agent takes into account how future state realizations will impact future parameter beliefs. Similar to the previous section, we

¹⁰We briefly summarize the mechanics of the asset pricing model as follows. If agents prefer an early resolution of uncertainty, changing beliefs are priced risks. Therefore, uncertainty about future revisions in beliefs leads to higher risk prices, equity premium, and return volatility.

¹¹Under this approach, the agent does not take into account future revisions in beliefs with respect to parameters, but she fully takes state uncertainty into account.

Figure 4: The role of learning in risk premium (under anticipated utility)



Notes: Risk premium is the expected excess return on consumption claim. RU indicates the case of preference for early resolution of uncertainty: $\gamma = 1.5, \psi = 1.5$. LU refers to the log utility case. We assume $\mu_1 = 0.84, \mu_2 = -0.22, \sigma_1^2 = 0.47, \sigma_2^2 = 0.56$ to compute the risk premium, which is provided in annualized percent term (y-axis). The length of the prior training sample is set to 8 periods. For $t - 1$ consecutive periods, we are in good state and receive good news. On t^{th} period, we are still in good state, but receive bad news. We consider $t \in \{4, 9\}$. We compare learning q and χ cases.

consider the experiment in which for $t - 1$ consecutive periods, the agent is in good state and receives good news. In the t^{th} period, she receives bad news while remaining in

the good state. We calculate the corresponding risk premium on a consumption claim under parameter learning with the anticipated utility assumption. We provide various cases with different prior means for q and χ and different values of t to understand the importance of prior beliefs and history dependence in this exercise.

Panels (A) and (B) of Figure 4 repeat the exercises shown in Panel (C) of Figure 2 for the risk premium under our $\gamma = 1.5, \psi = 1.5$ recursive utility calibration. Consistent with the results for forecast uncertainty, we find that the risk premium jumps up when bad news arrives and that the jump is larger when the bad news arrives after spending a longer time in the good state receiving good news. Also similarly to the case of forecast uncertainty, the jump is larger when agents learn about χ rather than about q .

Panels (C) and (D) show the same exercise under an alternate prior where $E(\chi) = 0.8$, $E(q) = 0.6$. In this case, the jumps are larger when agents learn about q rather than χ . In these exercises, the prior can be interpreted as the initial belief held by agents at the start of the simulation. Therefore, the differences seen under different priors is another illustration of the history-dependent nature of the asset price response to news in this economy. Panels (E) and (F) further illustrate this fact and we see that, overall, the effect of the bad news shock is larger for higher prior mean values of state persistence q and news accuracy χ .

Parameter learning also induces variations in risk premium during periods prior to the arrival of bad news, but the effect is minimal when prior beliefs about q and χ are high. This can be seen, for example, with high prior means $E(\chi) = 0.95$, $E(q) = 0.95$, a case which is provided in Panel (G). What is striking is the magnitude of the jump in the risk premium after the arrival of bad news: for example, in the case of learning q , the risk premium starts at 0.05% in period 1 and jumps to 0.77% with the arrival of bad news in period 9, roughly 15 times greater. It is important to emphasize that this is achieved with moderate values of $\gamma = 1.5, \psi = 1.5$. Without parameter learning, when beliefs about both q and χ remain at their prior values, the risk premium jumps to only 0.37% after the same sequence of state and news realizations, less than half of the size of risk premium with parameter learning. Also, when we repeat the exercise with log utility, displayed in Panel (H), the size of risk premium upon arrival of bad news significantly reduces to 0.03%. The size of the risk premium at period 9 is roughly 1.6 times greater than the value at period 1, a stark contrast to the massive amplification (15 times greater) achieved when learning about q is combined with a preference for early resolution of uncertainty. Overall, the optimism built during a long

period of economic expansion, i.e., the increase in posterior probability of remaining in the good state, can lead to a “Minsky moment” once the economic agent, endowed with a preference for early resolution of uncertainty, receives news indicating that the future is not as bright as expected. Parameter learning amplifies the effect of this news shock to generate a sudden increase in the risk premium despite no evidence of a recession in contemporaneous real growth rates.

One thing to note is that the risk premium associated with the case of learning q increases slightly over time as the economy remains in “good state, good news.” This is because we keep $q = q_{11} = q_{22}$ identical across states: as the agent stays in the good state for longer, she not only learns that the good state is more persistent, but that the bad state is more persistent as well. In a more realistic setting in which the agent believes persistence of the two states to differ and only learns about q_{11} , the risk premium decreases until period t as the agent remains in “good state, good news.” With the arrival of bad news, our simplifying assumption that $q_{11} = q_{22}$ also amplifies the magnitude of the jump in the risk premium. If only q_{11} is updated in this scenario, then when the bad news arrives, the agent puts roughly equal weight on an almost permanent good state and a slightly less persistent bad state. The corresponding risk premium jumps up by a lesser extent. However, in the more general case of $q_{11} \neq q_{22}$ when the agent only learns about q_{11} , the jump can be still larger for higher prior values of χ , q_{11} and q_{22} .

3 Estimation

3.1 Finding an empirical proxy for the news component

Our model features news that arrives in discrete form, but there is not a direct empirical proxy that has this feature. Instead, we look for a forward-looking variable that contains information about agents’ beliefs regarding future states. Imagine that there exist forecasters who know the true model parameters and current states, and in addition to this, receive noisy news about the future state. Let $I_t = \{n^t, S^t, y^t, \Pi, \theta\}$ denote the information set for these forecasters. Here, we are making the assumption that these forecasters are endowed with full structural knowledge of the economy, as in standard

rational expectations models. Suppose that we can observe their probability forecast¹²

$$z_t = p(S_{t+1} = 1|I_t). \quad (6)$$

The Survey of Professional Forecasters' anxious index, the probability of a decline in real GDP in the quarter after a survey is taken, is a reasonable real world proxy for (6). Professional forecasters have an information set that is closest to I_t , but in practice, it is possible that their information set may not be perfect. Their forecasts could be biased or inefficient. We allow for this by modeling the anxious index as

$$z_{\text{SPF},t} = \Phi\left(b_z + \Phi^{-1}\left(p(S_{t+1} = 1|I_t)\right) + u_t\right), \quad u_t \sim N(0, \sigma_z^2) \quad (7)$$

where $\Phi(\cdot)$ is a cdf of the standard normal distribution.¹³ Note that b_z and σ_z^2 capture potential bias and inefficiency in probability forecasts. If we set $b_z = \sigma_z^2 = 0$, then we recover (6). In the empirical analysis below, we proceed with the assumption that $b_z = 0$ but allow for errors with $\sigma_z^2 > 0$.

3.2 Information set

In Section 2, we used an assumption that some or all model parameters and the full history of states are known at time t to illustrate the implications of news for parameter learning, state prediction, forecast uncertainty, and asset returns. Here, in the econometrician's inference problem, this assumption is relaxed with all model parameters and states being unknown. Consider an econometrician who observes past and current output growth and recession probability forecasts. She updates her beliefs about states and parameters sequentially using Bayes' rule as she obtains new data.

3.3 Solving the econometrician's sequential learning problem

Formally, we develop a novel filtering technique that uses both actual GDP growth y_t and recession probability forecasts $z_{\text{SPF},t}$ from the Survey of Professional Forecasters to solve the sequential state filtering and parameter learning problem. Both observables

¹²Note that we could also use mean forecast, $E(y_{t+1}|I_t) = \sum_{i=1}^2 \mu_i p(S_{t+1} = i|I_t)$, which is a function of $p(S_{t+1} = i|I_t)$. Instead, we rely on a direct measure of $p(S_{t+1} = i|I_t)$.

¹³The choice of the probit linking function is just for convenience.

are collected in $x_t = [y_t, z_{\text{SPF},t}]$. Using data from 1969:Q1 to 2016:Q3, we obtain the full joint posterior distribution of the model primitives including the filtered distribution of discrete states at each time. The joint posterior $p(\theta, \Pi, \kappa^t | x^t)$ summarizes subjective beliefs after observing x^t . We use κ_t to indicate a realization of the combined Markov state $\kappa_t = \{S_t, n_t\}$ which can take on four values.

As explained by Johannes, Lochstoer, and Mou (2016), the joint learning of states and parameters is a high-dimensional problem which incurs confounding effects arising from multiple sources of uncertainty. We tackle this problem by relying on particle methods to directly sample from the particle approximation to the joint posterior, which can be factorized into the product of the conditional posteriors

$$p(\theta, \Pi, \kappa^t | x^t) = \underbrace{p(\theta, \Pi | \kappa^t, x^t)}_{\text{(i) parameter learning}} \times \underbrace{p(\kappa^t | x^t)}_{\text{(ii) state filtering}}. \quad (8)$$

To sample from (i) and (ii) jointly, we extend the particle learning algorithm developed by Carvalho, Johannes, Lopes, and Polson (2010), which is a generalization of the mixture Kalman filter of Chen and Liu (2000). The idea is to utilize conditional sufficient statistics for parameters and states as particles. The details are provided in Appendix C and Appendix E.

Before we move on to the application to the U.S. data, we conduct a simulation exercise to check the performance of the particle learning algorithm and examine how news embedded in survey forecasts influences the econometrician's sequential learning problem in the presence of multiple confounding effects.

3.4 Simulation exercise

In this exercise, we run the particle learning algorithm over different sets of simulated data. In all cases, we fix parameters at their prior median values in Table 2 and the length of simulated data is set to match the estimation sample. For all cases, we use the same set of simulated paths for output growth (y_t) and states (S_t) from equation (1). We simulate two different sets of time series of news (n_t): one in which news is informative $\chi = 0.8$ and the other in which it is not, that is $\chi = 0.5$. Survey forecasts ($z_{\text{SPF},t}$) are simulated based on (7) for each of these two cases of χ using the simulated states and the corresponding news series.

Table 1: Simulation: RMSE

| | Case 1 | | | Case 2 | | | Case 3 | | |
|------------------------|----------------------------|-------|-------|----------------------------|-------|-------|--------------|-------|-------|
| | $\chi = 0.5$ fix χ | | | $\chi = 0.8$ fix χ | | | learn χ | | |
| | 5% | 50% | 95% | 5% | 50% | 95% | 5% | 50% | 95% |
| Parameter learning | | | | | | | | | |
| μ_1 | 0.009 | 0.059 | 0.142 | 0.005 | 0.061 | 0.131 | 0.006 | 0.070 | 0.138 |
| σ_1^2 | 0.002 | 0.048 | 0.114 | 0.003 | 0.046 | 0.118 | 0.002 | 0.043 | 0.122 |
| μ_2 | 0.006 | 0.060 | 0.131 | 0.010 | 0.065 | 0.134 | 0.008 | 0.071 | 0.134 |
| σ_2^2 | 0.003 | 0.037 | 0.108 | 0.002 | 0.038 | 0.110 | 0.002 | 0.037 | 0.114 |
| q_{11} | 0.003 | 0.018 | 0.049 | 0.002 | 0.016 | 0.040 | 0.002 | 0.016 | 0.045 |
| q_{22} | 0.002 | 0.017 | 0.046 | 0.002 | 0.015 | 0.039 | 0.002 | 0.015 | 0.042 |
| Output growth forecast | | | | | | | | | |
| y_t | 0.656 | 0.727 | 0.783 | 0.628 | 0.694 | 0.750 | 0.629 | 0.693 | 0.752 |

Notes: We conduct three simulation exercises labeled by “Case 1, Case 2, Case 3.” In all data set, output growth data are assumed to be identical. The survey forecasts, however, are generated based on uninformative news $\chi = 0.5$ (Case 1) and informative news $\chi = 0.8$ (Case 2 and 3). In Case 1 and 2, we keep the number of estimated parameters to be identical by fixing χ and σ_z^2 to their true values. In Case 3, we learn all parameters including χ and σ_z^2 . In the top panel, we define $\text{RMSE} = \sqrt{\frac{1}{T} \sum_{t=1}^T (\theta - \theta_{t|1:t})^2}$ where θ denotes the true parameter value and $\theta_{t|1:t}$ is the posterior median estimate of θ conditional on information at t . In the bottom panel, we define $\text{RMSE} = \sqrt{\frac{1}{T-1} \sum_{t=2}^T (y_t - y_{t|1:t-1})^2}$ where $y_{t|1:t-1}$ is the posterior mean one-step-ahead prediction of y_t conditional on information at $t-1$. In the table we report 5%, 50%, 95% percentiles of RMSE distributions based on 100 Monte Carlo simulations.

For the particle learning algorithm, the details of conjugate prior distributions are provided in Table 2. We set the length of the prior training sample (prior precision) to 10 years. It is important to note that all simulation results are generated with unbiased priors.

In order to understand how news would influence the inference of other model parameters, We start by comparing two cases in which we keep the number of estimated parameters to be identical. Case 1 is the case in which news is uninformative and the econometrician correctly fixes χ to 0.5 in the estimation. In Case 2, news is informative ($\chi = 0.8$) and the econometrician fixes χ and σ_z^2 to their true values in the estimation and estimates the same set of parameters as in Case 1. Comparing these first two cases allows us to see how the presence of news shocks affects the econometricians learning problem while holding fixed the degree of parameter uncertainty. In Case 3, news is

informative as in Case 2, but the econometrician must now additionally learn χ and σ_z^2 . By comparing this case to Case 2, we aim to understand if parameter uncertainty with respect to news makes learning about the other parameters more difficult.

In the top panel of Table 1, we provide 5%, 50%, 95% percentiles of RMSE distributions based on 100 Monte Carlo simulations. The RMSE of parameter estimates is defined by $\sqrt{\frac{1}{T} \sum_{t=1}^T (\theta - \theta_{t|1:t})^2}$ where θ denotes the true parameter value and $\theta_{t|1:t}$ is the posterior median estimate of θ conditional on information at t . Two things are noteworthy. First, the small RMSEs across Monte Carlo simulations confirm the good performance of the particle learning algorithm. Second, we find roughly 10% improvement in parameter learning accuracy for q_{11} and q_{22} when news is informative. While the differences in absolute magnitudes are small, we find that RMSEs are uniformly smaller with informative news. The results for the other parameters are virtually identical across Cases 1 and 2. This is to be expected since we impose the same degree of uncertainty in both cases and news in this model is informative about the realization of the future state and not the distribution of growth conditional on a state. It is only when we learn parameters associated with news, i.e., χ and σ_z^2 in addition to the others, that we find some marginal deterioration of the econometrician's parameter learning accuracy for some parameters. The median RMSEs for μ_1 and μ_2 under Case 3 are larger than those in Case 2. The confounding nature of parameter learning is the key to understanding this result, which occurs when uncertainty about one object makes learning about the other more difficult.

In the bottom panel of Table 1, we compute output growth forecast RMSEs. We find a 5% improvement in the median ex-post accuracy of output growth forecasts if we allow purely forward-looking news to be embedded in probability forecasts, regardless of whether we fix or estimate χ and σ_z^2 . In sum, the simulation results are consistent with the implications of news derived in Section 2.

3.5 Application to U.S. data

We now apply the particle learning algorithm to U.S. data. We impose the same priors as in the simulation exercise.

Parameter estimates. Table 2 reports 5%, 50%, 95% percentiles of posterior distributions.¹⁴ The benchmark estimation results are provided in panel (2) of Table 2.

¹⁴The evolution of parameter learning is provided in Figure A-1. The credible intervals at time 0

Table 2: Prior and posterior distributions: Parameters

| | Prior (1) | | | Posterior | | | | | | | | |
|--------------|--------------|------|------|-----------|-------|------|------------------------------|-------|-------|-----------------|------|------|
| | | | | (2) | | | (3) | | | (4) | | |
| | | | | Benchmark | | | With surveys $\chi = 0.5$ | | | Without surveys | | |
| | 5% | 50% | 95% | 5% | 50% | 95% | 5% | 50% | 95% | 5% | 50% | 95% |
| μ_1 | -1.00 | 1.00 | 3.00 | 0.73 | 0.84 | 0.94 | 0.76 | 0.85 | 0.93 | 0.74 | 0.83 | 0.95 |
| σ_1^2 | 0.12 | 0.40 | 1.50 | 0.34 | 0.47 | 0.63 | 0.37 | 0.44 | 0.53 | 0.22 | 0.29 | 0.36 |
| μ_2 | -2.00 | 0.00 | 2.00 | -0.55 | -0.22 | 0.12 | -0.83 | -0.55 | -0.24 | 0.17 | 0.40 | 0.60 |
| σ_2^2 | 0.12 | 0.40 | 1.50 | 0.26 | 0.56 | 1.10 | 0.36 | 0.53 | 0.98 | 0.76 | 1.02 | 1.42 |
| q_{11} | 0.64 | 0.80 | 0.93 | 0.84 | 0.89 | 0.94 | 0.90 | 0.94 | 0.96 | 0.80 | 0.85 | 0.89 |
| q_{22} | 0.64 | 0.80 | 0.93 | 0.51 | 0.65 | 0.78 | 0.58 | 0.68 | 0.78 | 0.74 | 0.80 | 0.86 |
| χ | 0.64 | 0.80 | 0.93 | 0.84 | 0.91 | 0.96 | - | 0.50 | - | - | - | - |
| σ_z^2 | 0.06 | 0.24 | 0.96 | 0.39 | 0.71 | 1.28 | 0.28 | 0.35 | 0.42 | - | - | - |

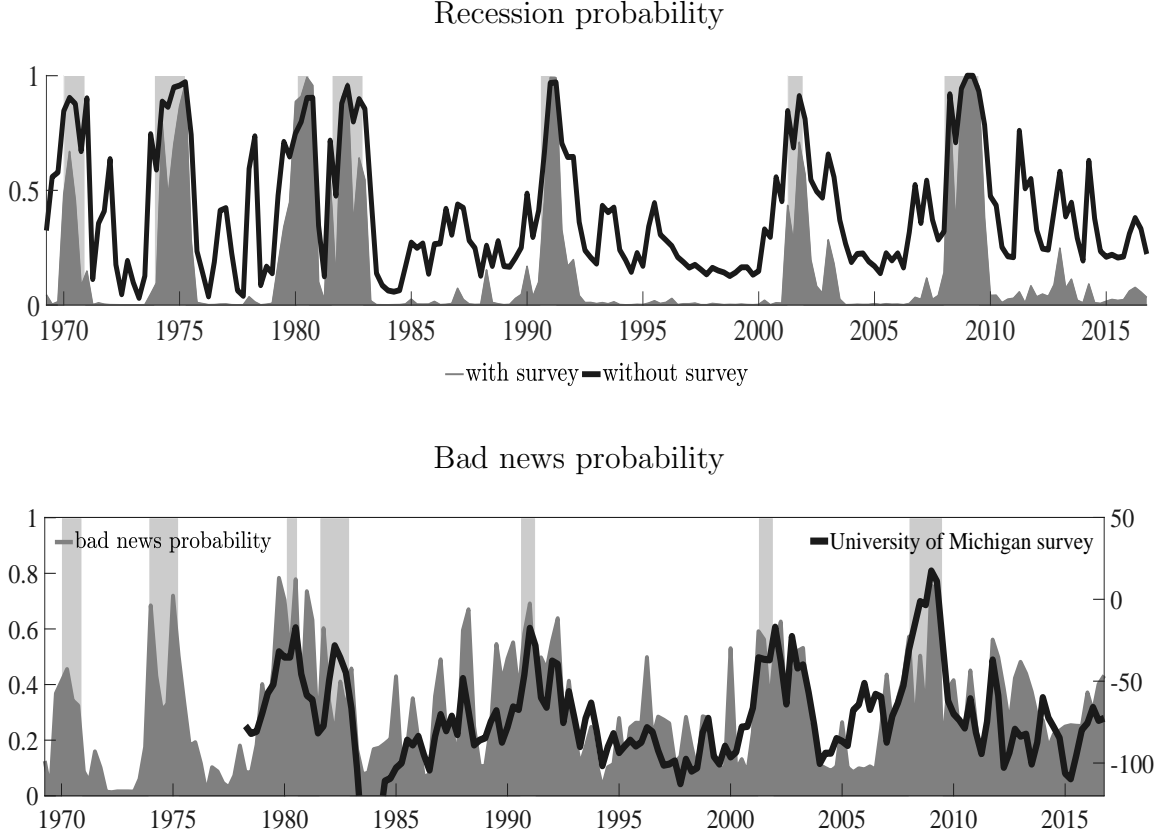
Notes: This table reports 5%, 50%, 95% percentiles of posterior distributions in Figure A-1. The details of prior choices are provided in Table A-1.

First, the first regime ($S_t = 1$) is identified with positive mean and the second regime ($S_t = 2$) with negative mean. Note that we only impose $\mu_1 > \mu_2$ to deal with the label switching problem in the estimation. We also find that posterior median estimate of variance is larger in the second regime than in the first regime which, together with mean estimates, provide the natural interpretation that the first regime is the expansion regime and the second regime is the recession regime. Second, the posterior intervals associated with the expansion regime are much tighter than those associated with the recession regime. This is not surprising because the average duration of expansions is much longer than the average duration of recessions, a property that is reflected in much lower estimates of q_{22} than q_{11} . Third, the posterior median estimate of χ is 0.91 which implies that news extracted from surveys are quite informative about the future regime.

To understand how news would influence the inference of model parameters, we repeat the estimation by fixing $\chi = 0.5$. The corresponding estimation results are provided in panel (3) of Table 2. We find that the posterior mean and variance estimates for the expansion regime are similar to those reported in panel (2). However, the mean estimates for the recession regime become more negative and both the mean and vari-

correspond to the 90% prior intervals. As more information from observed data is incorporated into the posterior distributions over time, the 90% credible intervals shrink. Those at time T are posterior credible intervals one would obtain from the entire times series of data.

Figure 5: Filtered estimates: State



Notes: In the top panel, we compare the two filtered recessions probabilities obtained with (gray area) and without surveys (black solid-line). In the bottom panel, the correlation of the model-implied $P(n_t = 2)$ (gray area) and the University of Michigan news index (black solid-line) is 0.60.

ance estimates in the recession regime are estimated with much more precision when we remove news from the estimation. Similarly, both state transition probabilities are slightly higher and estimated with more precision as well. Generally speaking, the width of the equal-tail probability 90% credible interval decreases for all parameters, highlighting that the confounding nature of learning news can potentially alter uncertainty associated with parameters as well. In this regard, this is consistent with the simulation exercise of Case 3 in Table 1.

Finally, we remove survey forecasts from the estimation to examine its impact on the inference of model parameters. Panel (4) of Table 2 reports posterior distributions from the estimation in which only output growth is used. We find that posterior median estimates associated with the recession regime are very different from those reported in

panels (2) and (3). Specifically, the posterior median estimate of μ_2 is positive and σ_2^2 is estimated to be twice larger. Perhaps surprisingly, q_{22} is estimated to be much more persistent without surveys. The distinction can be seen clearly in Figure A-1 in which the sequential parameter posterior distributions are plotted.

Regime probabilities. A different way to see the differences in the estimations with and without survey data is to look at the filtered regime probabilities.¹⁵ The top panel of Figure 5 combines the probabilities of “bad state, good news” and “bad state, bad news” and shows that this probability of the bad state roughly coincides with the NBER recession bars. However, when only output growth is used in the estimation (the “without survey” line), these recession probabilities tend to be biased upward and bad states are less tightly identified. This is reflected in the higher estimate of q_{22} in panel (4) of Table 2.

The bottom panel of Figure 5 combines the estimated probabilities of “good state, bad news” and “bad state, bad news” for our baseline case, giving the total probability of receiving bad news. It is interesting to observe that the correlation of the University of Michigan’s Survey of Consumers news index (inverted) and our filtered probability of bad news realizations is around 0.6.¹⁶ We also examine another measure of bad news that counts, for each quarter, the number of stories appearing in the New York Times and the Washington Post which include the word “recession”.¹⁷ We obtain a 0.47 correlation between our filtered probability of bad news and this index.

Forecasting GDP growth. We regress one-quarter ahead GDP growth on various explanatory variables including our estimated bad news probabilities (henceforth, bad news). We examine if the estimated news can predict one-period-ahead GDP growth as implied by the model. The regression results are provided in Table 3. As our model

¹⁵Figure A-2 provides the probability of each regime in the benchmark estimation. It is interesting to observe that the economy spends most of the time in the “good state, good news” regime. However, the probability of “good state, bad news” is non-negligible. This is the regime in which the economy is currently in the good state, but news suggests that the economy will enter bad state in the following period. On the other hand, the economy assigns very small probabilities to the “bad state, good news” and “bad state, bad news” regimes. Nevertheless, in periods where the probability of being in a bad state is high, the conditional probability of receiving good news can be substantial.

¹⁶This index is based on responses to the following question in the University of Michigan’s Survey of Consumers: “During the last few months, have you heard of any favorable or unfavorable changes in business conditions?” The index is constructed as the percent replying favorable minus the percent replying unfavorable plus 100. We compare the negative of this index to our filtered bad news probability.

¹⁷This is a replication of the R-word index developed by The Economist. A description can be found at <http://www.economist.com/node/566293>.

Table 3: Predicting GDP growth

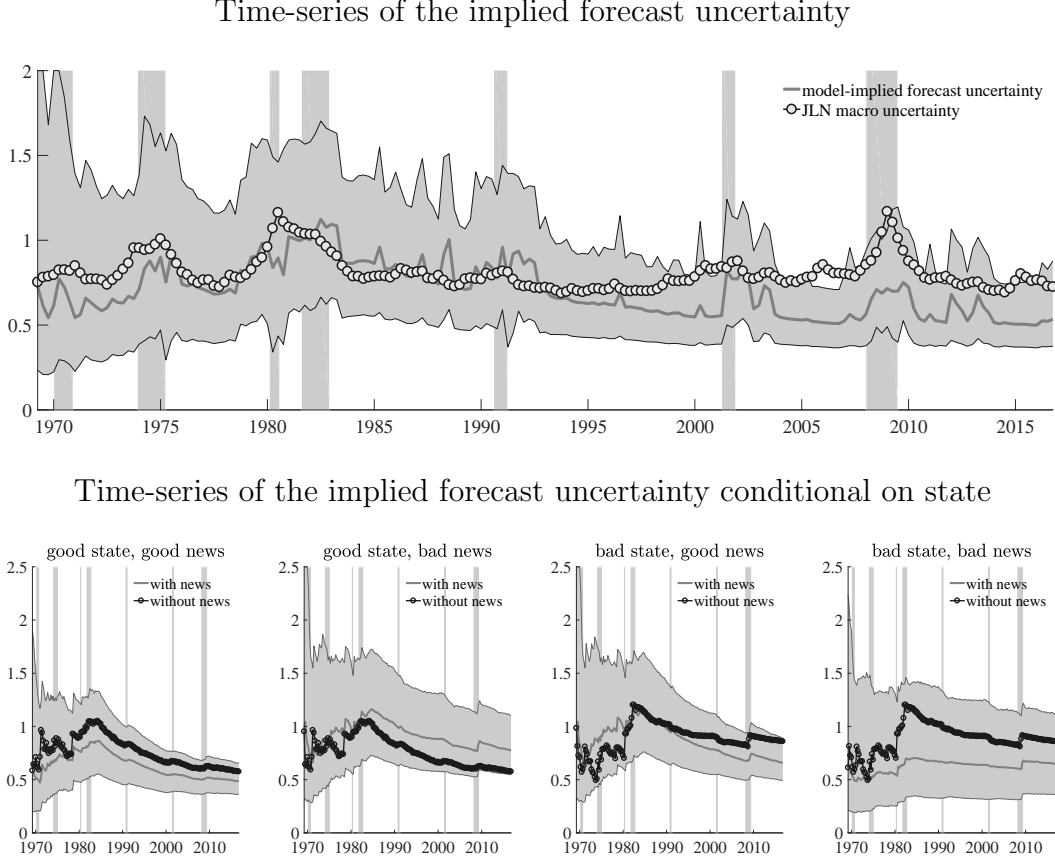
| | (A) | (B) | (C) | (D) | (E) |
|--------------------|----------------|-----------------|-----------------|-----------------|-----------------|
| constant | 0.45 (0.08) | 0.67 (0.05) | 0.54 (0.08) | 0.60 (0.08) | 0.40 (0.10) |
| current GDP growth | 0.32 (0.08) | | 0.20 (0.08) | 0.10 (0.09) | 0.37 (0.12) |
| bad news | | -0.34 (0.05) | -0.29 (0.07) | | |
| UMich survey | | | | -0.33 (0.07) | |
| r-word index | | | | | -0.04 (0.05) |
| adj- R^2 | 0.10 | 0.18 | 0.22 | 0.24 | 0.15 |

Notes: We regress one-quarter ahead GDP growth on various explanatory variables. Bad news refers to our estimated bad news probability. UMich survey is the University of Michigan bad news index. R-word index counts for each quarter how many stories that appear in the New York Times and the Washington Post include the word “recession.” The estimation sample for (A), (B), and (C) is from 1969:Q1 to 2016:Q3; the estimation sample for (D) is from 1978:Q1 to 2016:Q3; the estimation sample for (E) is from 1985:Q1 to 2016:Q3. The estimation results are qualitatively similar if we set the estimation sample identical across various specifications from 1985:Q1 to 2016:Q3. We report standard errors in parentheses. Since bad news is a generated regressor, asymptotic standard errors are constructed using generalized methods of moments.

predicts, bad news turns out to significantly predict lower future GDP growth and has strong forecasting power above the predictability contained in current GDP growth (compare across columns (A), (B), and (C)). We compare the forecasting power of our filtered bad news probability with other measures of bad news. We find that while the University of Michigan bad news index (column (D)) has the highest predictive power amongst all explanatory variables, the adjusted R^2 value is not too different from the value obtained from the benchmark prediction regression (column (C)). This is particularly notable in light of the fact that our bad news probabilities are filtered from professional forecasts collected during the middle month of a given quarter while both the University of Michigan survey and r-word index contain information collected throughout the entire quarter. This difference in timing should put these two alternate series at an advantage in forecasting relative to our bad news probabilities.

Forecast uncertainty. The top panel of Figure 6 plots the evolution of forecast error variance over time. The correlation between posterior median forecast error variance

Figure 6: Forecast uncertainty



Notes: In the top panel, we plot posterior median forecast error variance with the 90% credible interval (shaded areas). We compare with the macroeconomic uncertainty (circled-line) in Jurado, Ludvigson, and Ng (2015). The correlation between posterior median forecast error variance and JLN macro uncertainty is 0.49. In the bottom panel, we plot the conditional posterior median forecast error variance with the 90% credible interval (shaded areas). We compare with the conditional posterior median forecast error variance that assumes $\chi = 0.5$ (circled-line).

and the macroeconomic uncertainty in Jurado, Ludvigson, and Ng (2015) is 0.49.¹⁸ The bottom panel provides posterior forecast error variance conditional on each state, which is plotted against the median conditional posterior forecast error variance derived from the $\chi = 0.5$ (without news) case. Consistent with the implication in Figure 1, if news suggests that the current regime will persist next period, then forecast uncertainty monotonically decreases, i.e., the first and fourth column. On the contrary, if news con-

¹⁸It is important to note that Jurado, Ludvigson, and Ng (2015) provide an estimate of uncertainty that based on ex-post forecast errors. In our model, the relationship between ex-ante forecast error variance and the size of ex-post forecast errors is not monotonic since, as discussed in Section 2.2, news always reduces ex-post forecast errors while its relationship with ex-ante forecast variance is state-dependent.

tradicts the implication of the current state alone and suggests switching into a different state, then the weight is placed more equally on the two possible state outcomes. It turns out that for our full-sample posterior median estimates, forecast uncertainty increases with bad news in good states and decreases with good news in bad states, i.e., the second and third column.

4 Asset Pricing With Priced Parameter Uncertainty

Section 2.3 gave illustrative examples of the qualitative effects of news shocks on risk premia in the presence of parameter learning under the anticipated utility approach. While highly tractable, this approach abstracts from the pricing of risk due to parameter uncertainty. Instead, assets are priced as if the agent believes that her current mean estimates of parameter values are the true values. Collin-Dufresne, Johannes, and Lochstoer (2016) show that rationally pricing parameter uncertainty can lead to quantitatively large differences from the anticipated utility case. Therefore, in this section, we use the empirical estimates from Section 3 in a model where parameter uncertainty is rationally priced to assess the quantitative implications of our model for asset prices.

To be more precise, we solve an asset pricing problem that features fully rational sequential learning of unknown $\{q_{11}, q_{22}\}$ where the agent observes both the current true states as well as news about the one-period-ahead state.¹⁹ To alleviate the computational burden, we assume that the agent is fully aware of the rest of the model parameters including the accuracy of news.²⁰ One reason to allow the agent to learn $\{q_{11}, q_{22}\}$ rather than the other parameters is that uncertainty about transition probabilities has the largest asset pricing impact. Recall that we compared the implied risk premium under the case of learning news accuracy χ with the learning state persistence q case in Figure 4. For prior values of 0.8 or greater for both χ and q , we showed that learning q produced a larger jump in risk premia upon the arrival of bad news. From Collin-Dufresne, Johannes, and Lochstoer (2016), we also know that uncertainty about transition probabilities $\{q_{11}, q_{22}\}$ has a larger asset pricing impact than uncertainty

¹⁹Note that in our model, equilibrium asset prices reflect only information already available to the agent. Therefore, it is sufficient for her to learn parameters from only observations of the true states and news without explicitly considering asset prices to also be in her information set.

²⁰Each parameter that must be learned increases the number of state variables in the full-fledged parameter learning model. Therefore, the curse of dimensionality restricts us to consider learning over only a small number of parameters.

about conditional means or variances. Furthermore, as discussed in Section 3, since the news we are considering is about the future state and not about future growth rates, it only provides information about $\{q_{11}, q_{22}\}$ and not the other parameters governing the consumption or dividend processes in the model. Therefore, news in this model should interact more strongly with learning about $\{q_{11}, q_{22}\}$ than learning about $\{\mu_i, \sigma_i^2\}_{i=1,2}$.

4.1 The environment

Preferences. We continue to assume the same preferences represented by equation (4) which is repeated here for convenience,

$$V_t = \max_{C_t} \left[(1 - \beta) C_t^{\frac{1-\gamma}{\alpha}} + \beta (E_t V_{t+1}^{1-\gamma})^{\frac{1}{\alpha}} \right]^{\frac{\alpha}{1-\gamma}}. \quad (9)$$

Solution. The equilibrium expression for the wealth-consumption ratio is

$$PC(\kappa_t, X_t)^\alpha = E \left[\beta^\alpha e^{(1-\gamma)(\mu_{\kappa_{t+1}} + \sigma_{\kappa_{t+1}} \epsilon_{t+1})} (PC(\kappa_{t+1}, X_{t+1}) + 1)^\alpha | \kappa_t, X_t \right]$$

where X_t denotes summary statistics governing the parameter learning problem which evolve according to

$$X_{t+1} = f(\kappa_{t+1}, \kappa_t, X_t).$$

$E(q_{ii}|n^t, y^t, S^t, \theta)$ for $i \in \{1, 2\}$ are functions of $\{\kappa_t, X_t\}$ while $f(\cdot)$ is from Bayes' rule. The details are provided in Appendix A. Following Collin-Dufresne, Johannes, and Lochstoer (2016), we price an equity claim on an exogenous dividend that follows the growth process

$$\Delta d_{t+1} = \bar{\mu} + \rho(\Delta c_{t+1} - \bar{\mu}) + \sigma_d \epsilon_{d,t+1}, \quad \epsilon_{d,t+1} \sim N(0, 1), \quad (10)$$

and similarly solve for the price-dividend ratio of this claim. Here $\bar{\mu}$ is the unconditional mean of consumption growth. Its dependence on the state transition probabilities imply that the agent's beliefs about this quantity also evolve over time.

In this economy, the agent's beliefs about $\{q_{11}, q_{22}\}$ converge to the truth and her uncertainty about these parameters vanish as time progresses. Therefore, the model is solved by iterating the policy functions for both the wealth-consumption and price-dividend ratios backwards from a distant endpoint that is approximated by an economy

in which all parameters are known. Solutions for risk-free rates and risk premia are readily obtained from those for the wealth-consumption and price-dividend ratios. Details on the numerical solution algorithm are provided in Appendix F.

4.2 Model-implied asset prices

We simulate asset prices using the calibrated values in Johannes, Lochstoer, and Mou (2016)

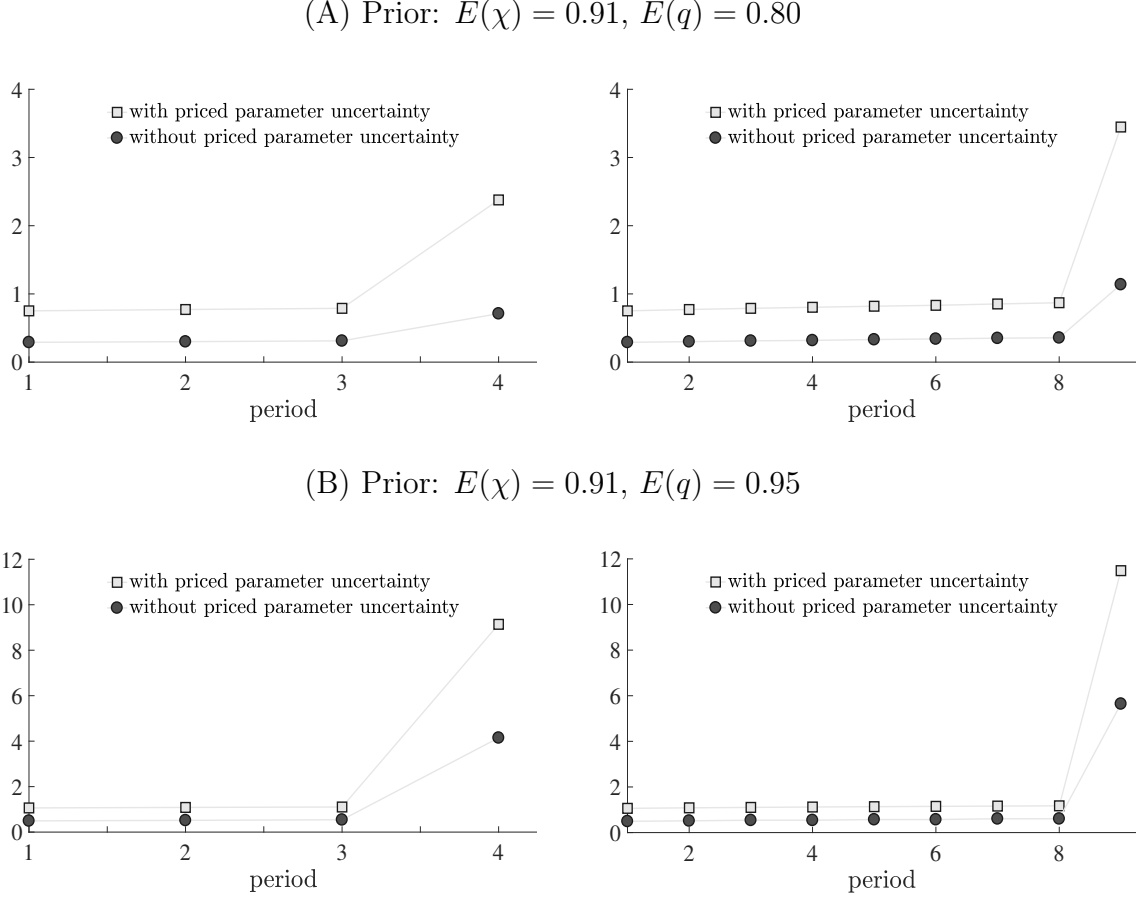
$$\beta = 0.994, \quad \gamma = 10, \quad \psi = 1.5, \quad \rho = 4.5, \quad \sigma_d = 4.81,$$

along with the “Benchmark” posterior median estimates of the growth and news process parameters in Table 2.

Quantitative effect of pricing parameter uncertainty. We first attempt to understand the quantitative effect of pricing parameter uncertainty on the risk premium of an agent compared to the anticipated utility case discussed in Section 2.3. For ease of comparison with Figure 4, we set $q = q_{11} = q_{22}$ and compute the expected excess return on a consumption claim.²¹ Figure 7 compares this consumption claim risk premium with parameter uncertainty to the one under anticipated utility as in Figure 4. Here, we set the prior value for news accuracy $\chi = 0.91$ and consider two prior values, 0.80 and 0.95, for state persistence q . As shown in the figure, we find a significant increase in the magnitude of risk premium jump upon the arrival of bad news when parameter uncertainty is priced. This is consistent with the finding in Collin-Dufresne, Johannes, and Lochstoer (2016) that parameter uncertainty gives rise to a quantitatively significant effect on asset prices. Compared to the value obtained under the anticipated utility approach, we find that the risk premium value is at least twice larger with priced parameter uncertainty. Consistent with the previous section, the quantitative difference is more apparent for a higher prior value for q . As in the anticipated utility case, we continue to see that bad news causes a larger jump in risk premia when it arrives after a longer expansion.

²¹Note that, for this example, we use the solution of the more general model described above where the agent believes that q_{11} and q_{22} can differ and her beliefs about these parameters follow separate Bayesian updating processes. However, to facilitate comparison with Figure 4, we exogenously set the path of q_{22} beliefs to be equal to that for q_{11} even though in our example, the agent should only learn q_{11} . In a model where the agent believes that a single parameter governs both transition probabilities, $q = q_{11} = q_{22}$, the parameter uncertainty and corresponding risk premia would likely be lower though our qualitative results should still hold.

Figure 7: The role of learning in risk premium on consumption claim



Notes: Risk premium is the expected excess return on consumption claim, which is derived under the case of preference for early resolution of uncertainty: $\gamma = 10$, $\psi = 1.5$. We solve an asset pricing problem that features fully rational sequential learning of unknown $q = q_{11} = q_{22}$. We compare with the risk premium value that does not account for parameter uncertainty. The numbers on y-axis are in annualized percent terms.

Simulated asset price moments. For the remainder of the paper, we revert to the more general case of learning separate transition probabilities $q_{11} \neq q_{22}$. We simulate asset prices based on the posterior parameter estimates in Table 2 along with the filtered states underlying Figure 5.²² In Table 4, we present moments from both the data as well as the 5th, 50th, and 95th percentiles of moments based on our model simulations.

²²The particle filter produces a set of draws from the posterior distribution at each point in time. It does not yield draws of complete time series from the posterior distribution. Therefore, these draws can be used to produce moments for ex-ante returns which depend only on current observations, but they cannot be used to compute ex-post returns which are a function of both current and lagged observations.

The table contains three cases. The first is our benchmark case while the second is a case without news shocks, which is equivalent to fixing $\chi = 0.5$ while keeping all other parameters the same. That is, the parameters used in both the “Benchmark” and $\chi = 0.5$ cases here come from the “Benchmark” posterior median estimates in Table 2. Likewise, both cases also use the same set of filtered states. Comparing these two cases isolates the effect of news shocks in this model conditional on our other benchmark parameters. The third case is one in which there are both no news shocks and all parameters governing the data-generating process of consumption are estimated without the use of survey data. That is, we use the “Without surveys” posterior median estimates in Table 2. We include this case because it features an estimation method commonly used to obtain parameter and regime estimates in many macroeconomic and asset pricing contexts. Comparing this case to the benchmark illustrates the role of news shocks while also highlighting how the change in inference from the addition of survey data affects asset prices.

Focusing first on the average risk-free rate and ex-ante equity premium, we see that adding news has some effect (though not large). The largest difference, in terms of these first two moments, actually comes from including survey data in the estimation. We see from the “Without surveys” case that, using the same set of asset pricing parameters but estimating the data-generating process of output using only real GDP growth data produces a higher average risk-free rate and a substantially lower average equity premium, particularly in the bad state. Given these asset pricing parameters, it is clear that the data-generating process estimated using both actual real GDP growth and recession probability forecasts does a better job of matching average risk-free rates and equity premia. Another interpretation of these results is that a researcher using a data-generating process estimated from only real GDP growth data would infer that an alternate set of asset pricing parameters is needed to match average risk-free rates and equity premia.

Next, we turn to volatilities of risk-free rates and equity premia. Now, it becomes clear that the main effect of allowing for moderately informative news in this asset pricing model is the amplification of these volatilities. The within-state volatility of the risk-free rate grows by 5.4 and 4.5 times in the good and bad states, respectively, relative to the case where news is irrelevant, thus bringing the model much closer to matching the data in this dimension. In terms of the equity premium, we see a similar amplification of volatility, particularly in the good state where the within-state standard deviation

Table 4: Asset pricing moments

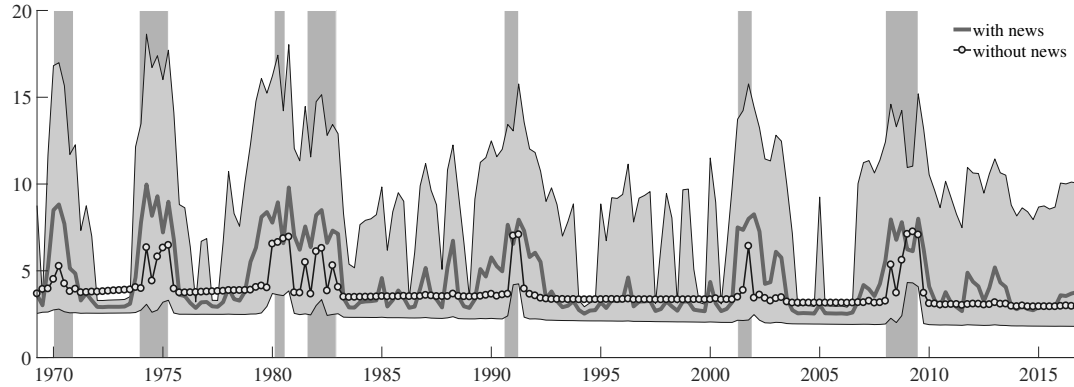
| | Data | With surveys | | | | | | Without surveys | | |
|--|------|--------------|------|-------|--------------|------|------|-----------------|------|------|
| | | Benchmark | | | $\chi = 0.5$ | | | | | |
| | | 5% | 50% | 95% | 5% | 50% | 95% | 5% | 50% | 95% |
| Average risk-free rate | | | | | | | | | | |
| Full sample | 0.93 | 3.22 | 3.57 | 3.78 | 3.25 | 3.36 | 3.47 | 3.79 | 3.84 | 3.89 |
| $S_t = 1$ | 1.04 | 3.49 | 3.79 | 3.96 | 3.60 | 3.67 | 3.71 | 4.19 | 4.20 | 4.22 |
| $S_t = 2$ | 0.44 | 1.41 | 2.33 | 2.94 | 1.31 | 1.64 | 2.02 | 3.29 | 3.30 | 3.33 |
| Average ex-ante equity premium | | | | | | | | | | |
| Full sample | 7.70 | 3.16 | 4.21 | 6.40 | 3.33 | 4.00 | 4.96 | 1.76 | 1.82 | 1.87 |
| $S_t = 1$ | 7.18 | 2.75 | 3.48 | 5.17 | 2.91 | 3.41 | 4.25 | 1.40 | 1.44 | 1.46 |
| $S_t = 2$ | 9.37 | 5.36 | 8.28 | 14.09 | 5.61 | 7.15 | 9.67 | 2.33 | 2.38 | 2.44 |
| Standard deviation of risk-free rate | | | | | | | | | | |
| Full sample | 1.96 | 0.93 | 1.08 | 1.31 | 0.60 | 0.74 | 0.86 | 0.43 | 0.44 | 0.46 |
| $S_t = 1$ | 1.81 | 0.81 | 0.97 | 1.19 | 0.15 | 0.18 | 0.21 | 0.04 | 0.05 | 0.06 |
| $S_t = 2$ | 2.36 | 0.39 | 0.72 | 0.96 | 0.05 | 0.16 | 0.30 | 0.04 | 0.05 | 0.06 |
| Standard deviation of ex-ante equity premium | | | | | | | | | | |
| Full sample | 2.35 | 1.67 | 2.85 | 5.17 | 0.99 | 1.42 | 2.06 | 0.46 | 0.48 | 0.51 |
| $S_t = 1$ | 2.00 | 1.28 | 2.16 | 3.98 | 0.15 | 0.32 | 0.56 | 0.06 | 0.07 | 0.10 |
| $S_t = 2$ | 2.59 | 1.05 | 2.61 | 5.76 | 0.39 | 0.81 | 1.86 | 0.12 | 0.15 | 0.19 |

Notes: We report the conditional averages of the log risk-free rate, log price-dividend ratio, and equity premium. We use the model-implied equity premium from Schorfheide, Song, and Yaron (2016). In the data, the conditional averages are computed based on expansion and recession states.

grows by over 6.7 times relative to the no news case. The model-implied conditional and unconditional equity premium standard deviations come quite close to matching the corresponding data moments.

This increase in volatilities of ex-ante returns follows from the effect of news on uncertainty that was highlighted in Section 2.2. In that section, for a simplified case with $q_{11} = q_{22}$, we show that news can increase uncertainty in switching states. Consistent with this intuition, we see that equity premia are higher in switching states, thus increasing equity premia volatility conditional on the growth state. The results from this simplified case, also suggest that when news contradicts the current growth state, equity premia are at their highest when $\chi = q$. Since our posterior estimates feature a χ that is much closer to q_{11} than q_{22} , this suggests that news shocks should increase equity premia volatility by more in the $S_t = 1$ growth state compared to the $S_t = 2$

Figure 8: Time-series of the equity premium



Notes: We provide the model-implied median equity premium with the 90% credible intervals (shaded-areas). We compare with the median equity premium computed without news (circled-line). We assume $\beta = 0.994$, $\gamma = 10$, $\psi = 1.5$, $\rho = 4.5$, and $\sigma_d = 4.81$. The numbers on y-axis are in annualized percent terms.

state. This is consistent with the results in Table 4.

Model-implied equity premium. Figure 8 provides the time-series of model-implied equity premium for our benchmark model and the case without news shocks. We find that allowing for new shocks produces an equity premium that fluctuates substantially more within recession and expansion periods. The additional volatility generated by news shocks is particularly prominent during the expansion of the late 1980s. It is also interesting to observe that our estimates indicate that bad news arriving prior to recessions often lead the model-implied equity premium to begin rising several quarters prior to the onset of recessions. For example, the equity premium soared from (roughly) 3% to 8% between 1978:Q2 and 1979:Q2 and remained there until the recession started in 1980:Q2. The benchmark model with news also generates a spike in equity premia in 1987:Q4 and 1988:Q1 which corresponds to the Black Monday crash. Even though we do not include asset prices directly in the estimation, the survey recession probabilities in these periods reflect an economic outlook darkened by the stock market crash. Our estimation interprets this as a heightened filtered probability of bad news about future GDP growth, as can be seen in Figure 5, which produces a high equity premium in these periods despite contemporaneous GDP growth remaining high. The fact that this bad news arrived when the economy had been in expansion for quite some time amplified its effect on equity premia, a scenario that can be described as a “Minsky moment”.²³

²³Relative to a model with only Gaussian growth and news shocks, this increase in the equity

The equity premia generated without news do not have these features.

5 Conclusion

Economic agents consider not only current fundamentals but also news when forming beliefs about the future. In this paper, we study the channels through which news influences subjective beliefs of economic agents, with particular focus on their subjective uncertainty. In a two-state Markov-switching economy, we consider an agent who receives news each period that reveals the next period’s state with some error. We show that when news contradicts existing beliefs, the agent’s beliefs are revised toward a uniform distribution, raising subjective uncertainty. When the agent rationally learns model parameters, the response of uncertainty to news depends on not just current, but also past, states. In this environment, parameter learning introduces additional state variables to the model that summarize information from past states and alters the effects of news on agent’s beliefs.

In light of these properties of our model, we examine the extent to which news-driven uncertainty fluctuations can generate variation in asset prices. We show that the optimism built during a long period of economic boom, i.e., the increase in the believed probability of remaining in the good state, can trigger a “Minsky moment” once the agent suddenly receives news that the future may not be as bright as expected. The effect is greater the longer the expansion has lasted, the higher the prior beliefs about state persistence or news accuracy, and when the agent has preference for early resolution of uncertainty.

Using a novel filtering technique, we estimate the model using recession probability forecasts from the Survey of Professional Forecasters. Our filtered probability of bad news correlates strongly with survey- and media-based measures and strongly negatively predicts one-step ahead GDP growth after controlling for current GDP growth as implied by the model. Posterior beliefs vary significantly over time with bad news frequently raising uncertainty during expansions.

Based on model estimates, we assess our model’s quantitative implications for asset prices in a setting where the agent prefers an early resolution of uncertainty. We show

premium is also amplified by the increase in uncertainty when bad news contradicts the current high growth state.

that the main effect of allowing for informative news in this asset pricing model is the amplification of asset return volatilities: This is because news can increase uncertainty when it contradicts the agent's existing beliefs. In sum, news shocks greatly improve the model's ability to match both conditional and unconditional moments in the data. Finally, we identify historical periods in which equity premia were elevated due to news.

References

- ANDERSEN, T., T. BOLLERSLEV, F. DIEBOLD, AND C. VEGA (2007): “Real-time price discovery in global stock, bond and foreign exchange markets,” *Journal of International Economics*, 73(2), 251–277.
- BANSAL, R., AND A. YARON (2004): “Risks For the Long Run: A Potential Resolution of Asset Pricing Puzzles,” *Journal of Finance*, 59, 1481–1509.
- BARSKY, R., AND E. SIMS (2011): “News Shocks and Business Cycles,” *Journal of Monetary Economics*, 58(3), 273–289.
- BEAUDRY, P., AND F. PORTIER (2006): “Stock Prices, News, and Economic Fluctuations,” *American Economic Review*, 96(4), 1293–1307.
- BEAUDRY, P., AND F. PORTIER (2014): “News-Driven Business Cycles: Insights and Challenges,” *Journal of Economic Literature*, 52(4), 993–1074.
- BERGER, D., I. DEW-BECKER, AND S. GIGLIO (2017): “Uncertainty Shocks as Second-moment News Shocks,” Manuscript.
- BOYD, J., J. HU, AND R. JAGANNATHAN (2005): “The Stock Market’s Reaction to Unemployment News: Why Bad News is Usually Good for Stocks,” *Journal of Finance*, 60, 649–672.
- CARVALHO, C., M. JOHANNES, H. LOPES, AND N. POLSON (2010): “Particle Learning and Smoothing,” *Statistical Science*, 25(1), 88–106.
- CHEN, R., AND J. LIU (2000): “Mixture Kalman Filters,” *Journal of the Royal Statistical Society Series B*, 62, 493–508.
- COLLIN-DUFRESNE, P., M. JOHANNES, AND L. LOCHSTOER (2016): “Parameter Learning in General Equilibrium: The Asset Pricing Implications,” *American Economic Review*, 106(3), 664–698.
- CONSTANTINIDES, G., AND A. GHOSH (2016): “What Information Drives Asset Prices?,” Manuscript.
- EPSTEIN, L., AND S. ZIN (1989): “Substitution, Risk Aversion and the Temporal Behavior of Consumption and Asset Returns: A Theoretical Framework,” *Econometrica*, 57, 937–969.

- FAUST, J., R. J. W. S., AND J. WRIGHT (2007): “The High-Frequency Response of Exchange Rates and Interest Rates to Macroeconomic Announcements,” Board of Governors of the Federal Reserve System International Finance Discussion Papers 784.
- GURKAYNAK, R., B. SACK, AND E. SWANSON (2005): “The excess sensitivity of long-term interest rates: evidence and implications for macroeconomic models,” *American Economic Review*, 95(1), 425–36.
- HIROSE, Y., AND T. KUROZUMI (2012): “Identifying News Shocks with Forecast Data,” *CAMA Working Paper 1/2012*.
- JAIMOVICH, N., AND S. REBELO (2009): “Can News about the Future Drive the Business Cycle?,” *American Economic Review*, 99(4), 1097–1118.
- JOHANNES, M., L. LOCHSTOER, AND Y. MOU (2016): “Learning about Consumption Dynamics,” *Journal of Finance*, 71, 551–600.
- JURADO, K., S. LUDVIGSON, AND S. NG (2015): “Measuring Uncertainty,” *American Economic Review*, 105(3), 1177–1216.
- KOZENIAUSKAS, N., A. ORLIK, AND L. VELDKAMP (2016): “The Common Origin of Uncertainty Shocks,” Working Paper 22384, National Bureau of Economic Research, DOI: 10.3386/w22384.
- KURMANN, A., AND C. OTROK (2013): “News Shocks and the Slope of the Term Structure of Interest Rates,” *American Economic Review*, 103(6), 2612–32.
- LUCCA, D., AND E. MOENCH (2015): “The Pre-FOMC Announcement Drift,” *Journal of Finance*, 70, 329–371.
- MALKHOZOV, A., AND A. TAMONI (2015): “News Shocks and Asset Prices,” Manuscript.
- MILANI, F., AND A. RAJRHANDARI (2012): “Observed Expectations, News Shocks, and the Business Cycle,” Manuscript.
- MIYAMOTO, W., AND T. L. NGUYEN (2015): “News Shocks and Business Cycles: Evidence from Forecast Data,” SSRN Scholarly Paper ID 2496739, Social Science Research Network, Rochester, NY.

- SAVOR, P., AND M. WILSON (2013): “How Much Do Investors Care About Macroeconomic Risk? Evidence from Scheduled Economic Announcements,” *Journal of Financial and Quantitative Analysis*, 48, 343–375.
- SCHMITT-GROHE, S., AND M. URIBE (2012): “Whats News in Business Cycles,” *Econometrica*, 80(6), 2733–2764.
- SCHORFHEIDE, F., D. SONG, AND A. YARON (2016): “Identifying Long-Run Risks: A Bayesian Mixed-Frequency Approach,” Manuscript.
- TANG, J. (2017): “FOMC Communication and Interest Rate Sensitivity to News,” Manuscript.
- VERONESI, P. (1999): “Stock Market Overreaction to Bad News in Good Times: A Rational Expectations Equilibrium Model,” *Review of Financial Studies*, 12(5), 975–1007.

Online Appendix:

News-Driven Uncertainty Fluctuations

Dongho Song and Jenny Tang

A Posterior of the Markov-Transition Probabilities

A.1 Without news

Prior. At $t = 0$, the agent is given an initial (potentially truncated) Beta-distributed prior over each of these parameters and thereafter updates beliefs sequentially upon observing the time-series of realized regimes, S_t .

$$\begin{aligned} p(\Pi|\theta) &= p(q_{11})p(q_{22}) \\ &\propto q_{11}^{a_{1,0}-1}(1-q_{11})^{b_{1,0}-1}q_{22}^{a_{2,0}-1}(1-q_{22})^{b_{2,0}-1} \end{aligned} \quad (\text{A-1})$$

where $\{a_{1,0}, b_{1,0}, a_{2,0}, b_{2,0}\}$ can be interpreted as observations from a training sample of $a_{1,0} + b_{1,0} + a_{2,0} + b_{2,0} - 4$ periods which contained $a_{i,0} - 1$ observations of state i to state i transitions and $b_{i,0} - 1$ observations of state i to state $j \neq i$ transitions.

Likelihood. The binomial likelihood is

$$p(S^t|\Pi, \theta) = q_{11}^{a_{1,t}-a_{1,0}-1}(1-q_{11})^{b_{1,t}-b_{1,0}-1}q_{22}^{a_{2,t}-a_{2,0}-1}(1-q_{22})^{b_{2,t}-b_{2,0}-1}. \quad (\text{A-2})$$

Observations. The standard Bayes rule shows that the updating equations count the number of times state i has been followed by state i versus the number of times state i has been followed by state j .

$$\begin{aligned} a_{i,t} &= a_{i,0} + \# (\text{state } i \text{ has been followed by state } i), \\ b_{i,t} &= b_{i,0} + \# (\text{state } i \text{ has been followed by state } j). \end{aligned} \quad (\text{A-3})$$

The law of motions for $a_{i,t}$ and $b_{i,t}$ are

$$\begin{aligned} a_{i,t+1} &= a_{i,t} + \mathbb{I}_{\{S_{t+1}=i\}}\mathbb{I}_{\{S_t=i\}} \\ b_{i,t+1} &= b_{i,t} + (1 - \mathbb{I}_{\{S_{t+1}=i\}})\mathbb{I}_{\{S_t=i\}}. \end{aligned} \quad (\text{A-4})$$

Posterior. The prior Beta-distribution coupled with the realization of regimes leads to a conjugate prior and so posterior beliefs are also Beta-distributed. Using this prior (A-1) and the binomial likelihood (A-2) associated with observations $\{a_{1,t}, b_{1,t}, a_{2,t}, b_{2,t}\}_{t=1}^T$, the posterior is

$$\begin{aligned}
 p(\Pi|y^t, S^t, \theta) &= \frac{p(y^t, S^t|\Pi, \theta)p(\Pi|\theta)}{p(y^t, S^t|\theta)} \\
 &= \frac{p(y^t|S^t, \Pi, \theta)p(S^t|\Pi, \theta)p(\Pi|\theta)}{p(y^t|S^t, \theta)p(S^t|\theta)} \\
 &= \frac{p(S^t|\Pi, \theta)p(\Pi|\theta)}{p(S^t|\theta)} \quad \text{since } p(y^t|S^t, \Pi, \theta) = p(y^t|S^t, \theta) \\
 &= \frac{q_{11}^{a_{1,t}-1}(1-q_{11})^{b_{1,t}-1}q_{22}^{a_{2,t}-1}(1-q_{22})^{b_{2,t}-1}}{B(a_{1,t}, b_{1,t})B(a_{2,t}, b_{2,t})}.
 \end{aligned} \tag{A-5}$$

From (A-1) and (A-2)

$$\begin{aligned}
 p(S^t|\theta) &= \int p(S^t|\Pi, \theta)p(\Pi|\theta)d\Pi \\
 &= \int q_{11}^{a_{1,t}-1}(1-q_{11})^{b_{1,t}-1}dq_{11} \int q_{22}^{a_{2,t}-1}(1-q_{22})^{b_{2,t}-1}dq_{22} \\
 &= B(a_{1,t}, b_{1,t})B(a_{2,t}, b_{2,t}).
 \end{aligned} \tag{A-6}$$

Posterior (A-5) is independent and equal to

$$\begin{aligned}
 p(\Pi|y^t, S^t, \theta) &= p(q_{11}|y^t, S^t, \theta) \cdot p(q_{22}|y^t, S^t, \theta) \\
 &= p(q_{11}|S^t, \theta) \cdot p(q_{22}|S^t, \theta) \\
 &= \frac{q_{11}^{a_{1,t}-1}(1-q_{11})^{b_{1,t}-1}}{B(a_{1,t}, b_{1,t})} \cdot \frac{q_{22}^{a_{2,t}-1}(1-q_{22})^{b_{2,t}-1}}{B(a_{2,t}, b_{2,t})},
 \end{aligned} \tag{A-7}$$

and the posterior means are

$$\begin{aligned}
E(q_{11}|y^t, S^t, \theta) &= \int q_{11} p(\Pi|y^t, S^t, \theta) d\Pi \\
&= \int \frac{q_{11}^{a_{1,t}} (1 - q_{11})^{b_{1,t}-1}}{B(a_{1,t}, b_{1,t})} dq_{11} \int \frac{q_{22}^{a_{2,t}} (1 - q_{22})^{b_{2,t}-1}}{B(a_{2,t}, b_{2,t})} dq_{22} \\
&= \frac{B(a_{1,t} + 1, b_{1,t})}{B(a_{1,t}, b_{1,t})} \\
&= \frac{a_{1,t}}{a_{1,t} + b_{1,t}} \\
E(q_{22}|y^t, S^t, \theta) &= \frac{a_{2,t}}{a_{2,t} + b_{2,t}}
\end{aligned} \tag{A-8}$$

where the last two lines follow from the definition of beta and gamma distribution

- $p(y) = \frac{y^{\alpha-1}(1-y)^{\beta-1}}{B(\alpha, \beta)}$ for $0 \leq y \leq 1$
- $B(\alpha, \beta) = \frac{\Gamma(\alpha)\Gamma(\beta)}{\Gamma(\alpha+\beta)}$
- $\Gamma(\alpha + n) = \frac{(\alpha+n-1)!}{(\alpha-1)!} \Gamma(\alpha)$
- $E(y^n) = \frac{B(\alpha+n, \beta)}{B(\alpha, \beta)} = \frac{\Gamma(\alpha+n)\Gamma(\alpha+\beta)}{\Gamma(\alpha+\beta+n)\Gamma(\alpha)}$.

A.2 With news

We can compute

$$p(S^t|\Pi, \theta)p(\Pi|\theta) = q_{11}^{a_{1,t}-1}(1 - q_{11})^{b_{1,t}-1} q_{22}^{a_{2,t}-1}(1 - q_{22})^{b_{2,t}-1} \tag{A-9}$$

and

$$\begin{aligned}
p(n_t|S^t, \Pi, \theta) &= \sum_{S_{t+1} \in \{1,2\}} p(n_t|S_{t+1}, S^t, \Pi, \theta) p(S_{t+1}|S^t, \Pi, \theta) \\
&= \begin{cases} \chi q_{11} + (1 - \chi)(1 - q_{11}) = 1 - \chi + (2\chi - 1)q_{11}, & \text{if } n_t = 1, S_t = 1 \\ (1 - \chi)q_{11} + \chi(1 - q_{11}) = \chi - (2\chi - 1)q_{11}, & \text{if } n_t = 2, S_t = 1 \end{cases}
\end{aligned} \tag{A-10}$$

and from (A-9), (A-10),

$$\begin{aligned}
 p(n_t, S^t | \theta) &= \int p(n_t | S^t, \Pi, \theta) p(S^t | \Pi, \theta) p(\Pi | \theta) d\Pi \\
 &= \begin{cases} \left(1 - \chi + (2\chi - 1) \frac{a_{1,t}}{a_{1,t} + b_{1,t}}\right) B(a_{1,t}, b_{1,t}) B(a_{2,t}, b_{2,t}), & \text{if } n_t = 1, S_t = 1 \\ \left(1 - \chi + (2\chi - 1) \frac{b_{1,t}}{a_{1,t} + b_{1,t}}\right) B(a_{1,t}, b_{1,t}) B(a_{2,t}, b_{2,t}), & \text{if } n_t = 2, S_t = 1. \end{cases}
 \end{aligned} \tag{A-11}$$

From (A-11), we can deduce that the conditional posterior distribution of the Markov-switching transition probability matrix is

$$\begin{aligned}
 p(\Pi | n_t, y^t, S^t, \theta) &= p(\Pi | n_t, S^t, \theta) = p(q_{11} | n_t, S^t, \theta) p(q_{22} | n_t, S^t, \theta) \\
 &= \begin{cases} \frac{(1-\chi+(2\chi-1)q_{11})}{(1-\chi+(2\chi-1)\frac{a_{1,t}}{a_{1,t}+b_{1,t}})} \cdot \frac{q_{11}^{a_{1,t}-1}(1-q_{11})^{b_{1,t}-1}}{B(a_{1,t}, b_{1,t})} \cdot \frac{q_{22}^{a_{2,t}-1}(1-q_{22})^{b_{2,t}-1}}{B(a_{2,t}, b_{2,t})}, & \text{if } n_t^1 = 1, S_t = 1 \\ \frac{q_{11}^{a_{1,t}-1}(1-q_{11})^{b_{1,t}-1}}{B(a_{1,t}, b_{1,t})} \cdot \frac{(1-\chi+(2\chi-1)q_{22})}{(1-\chi+(2\chi-1)\frac{a_{2,t}}{a_{2,t}+b_{2,t}})} \cdot \frac{q_{22}^{a_{2,t}-1}(1-q_{22})^{b_{2,t}-1}}{B(a_{2,t}, b_{2,t})}, & \text{if } n_t^1 = 2, S_t = 2 \\ \frac{(1-\chi+(2\chi-1)(1-q_{11}))}{(1-\chi+(2\chi-1)\frac{b_{1,t}}{a_{1,t}+b_{1,t}})} \cdot \frac{q_{11}^{a_{1,t}-1}(1-q_{11})^{b_{1,t}-1}}{B(a_{1,t}, b_{1,t})} \cdot \frac{q_{22}^{a_{2,t}-1}(1-q_{22})^{b_{2,t}-1}}{B(a_{2,t}, b_{2,t})}, & \text{if } n_t^1 = 2, S_t = 1 \\ \frac{q_{11}^{a_{1,t}-1}(1-q_{11})^{b_{1,t}-1}}{B(a_{1,t}, b_{1,t})} \cdot \frac{(1-\chi+(2\chi-1)(1-q_{22}))}{(1-\chi+(2\chi-1)\frac{b_{2,t}}{a_{2,t}+b_{2,t}})} \cdot \frac{q_{22}^{a_{2,t}-1}(1-q_{22})^{b_{2,t}-1}}{B(a_{2,t}, b_{2,t})}, & \text{if } n_t^1 = 1, S_t = 2. \end{cases}
 \end{aligned} \tag{A-12}$$

The posterior means are

$$E(q_{11} | n_t^1, y^t, S^t, \theta) = \begin{cases} \frac{\chi(a_{1,t}+1)+(1-\chi)b_{1,t}}{\chi a_{1,t}+(1-\chi)b_{1,t}} \cdot \frac{a_{1,t}}{a_{1,t}+b_{1,t}+1}, & \text{if } n_t^1 = 1, S_t = 1 \\ \frac{(1-\chi)(a_{1,t}+1)+\chi b_{1,t}}{(1-\chi)a_{1,t}+\chi b_{1,t}} \cdot \frac{a_{1,t}}{a_{1,t}+b_{1,t}+1}, & \text{if } n_t^1 = 2, S_t = 1 \\ \frac{a_{1,t}}{a_{1,t}+b_{1,t}}, & \text{if } n_t^1 \in \{1, 2\}, S_t = 2 \end{cases}$$

and

$$E(q_{22} | n_t^1, y^t, S^t, \theta) = \begin{cases} \frac{\chi(a_{2,t}+1)+(1-\chi)b_{2,t}}{\chi a_{2,t}+(1-\chi)b_{2,t}} \cdot \frac{a_{2,t}}{a_{2,t}+b_{2,t}+1}, & \text{if } n_t^1 = 2, S_t = 2 \\ \frac{(1-\chi)(a_{2,t}+1)+\chi b_{2,t}}{(1-\chi)a_{2,t}+\chi b_{2,t}} \cdot \frac{a_{2,t}}{a_{2,t}+b_{2,t}+1}, & \text{if } n_t^1 = 1, S_t = 2 \\ \frac{a_{2,t}}{a_{2,t}+b_{2,t}}, & \text{if } n_t^1 \in \{1, 2\}, S_t = 1. \end{cases}$$

To calculate the posterior variances, we need $E(q_{ii}^2|n_t^1, y^t, S^t, \theta) - (E(q_{ii}|n_t^1, y^t, S^t, \theta))^2$

$$E(q_{11}^2|n_t^1, y^t, S^t, \theta) = \begin{cases} \frac{\chi(a_{1,t}+2)+(1-\chi)b_{1,t}}{\chi a_{1,t}+(1-\chi)b_{1,t}} \frac{a_{1,t}}{a_{1,t}+b_{1,t}+1} \frac{a_{1,t}+1}{a_{1,t}+b_{1,t}+2}, & \text{if } n_t^1 = 1, S_t = 1 \\ \frac{(1-\chi)(a_{1,t}+2)+\chi b_{1,t}}{(1-\chi)a_{1,t}+\chi b_{1,t}} \frac{a_{1,t}}{a_{1,t}+b_{1,t}+1} \frac{a_{1,t}+1}{a_{1,t}+b_{1,t}+2}, & \text{if } n_t^1 = 2, S_t = 1 \\ \frac{a_{1,t}}{a_{1,t}+b_{1,t}} \frac{a_{1,t}+1}{a_{1,t}+b_{1,t}+1}, & \text{if } n_t^1 \in \{1, 2\}, S_t = 2 \end{cases}$$

and

$$E(q_{22}^2|n_t^1, y^t, S^t, \theta) = \begin{cases} \frac{\chi(a_{2,t}+2)+(1-\chi)b_{2,t}}{\chi a_{2,t}+(1-\chi)b_{2,t}} \frac{a_{2,t}}{a_{2,t}+b_{2,t}+1} \frac{a_{2,t}+1}{a_{2,t}+b_{2,t}+2}, & \text{if } n_t^1 = 2, S_t = 2 \\ \frac{(1-\chi)(a_{2,t}+2)+\chi b_{2,t}}{(1-\chi)a_{2,t}+\chi b_{2,t}} \frac{a_{2,t}}{a_{2,t}+b_{2,t}+1} \frac{a_{2,t}+1}{a_{2,t}+b_{2,t}+2}, & \text{if } n_t^1 = 1, S_t = 2 \\ \frac{a_{2,t}}{a_{2,t}+b_{2,t}} \frac{a_{2,t}+1}{a_{2,t}+b_{2,t}+1}, & \text{if } n_t^1 \in \{1, 2\}, S_t = 1. \end{cases}$$

B The State Transition Probability

We compute the state transition probabilities

$$p(S_{t+1}, n_{t+1}|S_t, n_t, y_t, \Pi, \theta) = p(n_{t+1}|S_{t+1}, S_t, n_t, y_t, \Pi, \theta)p(S_{t+1}|S_t, n_t, y_t, \Pi, \theta). \quad (\text{A-13})$$

The first component of (A-13) can be expressed by

$$\begin{aligned} p(n_{t+1}|S_{t+1}, S_t, n_t, y_t, \Pi, \theta) &= \sum_{S_{t+2}} p(n_{t+1}|S_{t+2}, S_{t+1}, S_t, n_t, y_t, \Pi, \theta)p(S_{t+2}|S_{t+1}, S_t, n_t, y_t, \Pi, \theta) \\ &= \sum_{S_{t+2}} p(n_{t+1}|S_{t+2}, \Pi, \theta)p(S_{t+2}|S_{t+1}, \Pi, \theta) \\ &= \begin{cases} (1-\chi) + (2\chi-1)q_{11}, & \text{if } S_{t+1} = 1, n_{t+1} = 1 \\ \chi - (2\chi-1)q_{11}, & \text{if } S_{t+1} = 1, n_{t+1} = 2 \\ \chi - (2\chi-1)q_{22}, & \text{if } S_{t+1} = 2, n_{t+1} = 1 \\ (1-\chi) + (2\chi-1)q_{22}, & \text{if } S_{t+1} = 2, n_{t+1} = 2. \end{cases} \end{aligned}$$

The second component of (A-13) can be expressed by

$$\begin{aligned}
 p(S_{t+1}|n_t, S^t, \Pi, \theta) &= \frac{p(n_t|S_{t+1}, S^t, \Pi, \theta)p(S_{t+1}|S^t, \Pi, \theta)}{p(n_t|S_t, \Pi, \theta)} \\
 &= \begin{cases} \frac{\chi q_{11}}{(1-\chi)+(2\chi-1)q_{11}}, & \text{if } n_t = 1, S_t = 1, S_{t+1} = 1 \\ \frac{(1-\chi)(1-q_{11})}{(1-\chi)+(2\chi-1)q_{11}}, & \text{if } n_t = 1, S_t = 1, S_{t+1} = 2 \\ \frac{(1-\chi)q_{11}}{\chi-(2\chi-1)q_{11}}, & \text{if } n_t = 2, S_t = 1, S_{t+1} = 1 \\ \frac{\chi(1-q_{11})}{\chi-(2\chi-1)q_{11}}, & \text{if } n_t = 2, S_t = 1, S_{t+1} = 2, \end{cases} \\
 &= \begin{cases} \frac{\chi(1-q_{22})}{\chi-(2\chi-1)q_{22}}, & \text{if } n_t = 1, S_t = 2, S_{t+1} = 1 \\ \frac{(1-\chi)q_{22}}{\chi-(2\chi-1)q_{22}}, & \text{if } n_t = 1, S_t = 2, S_{t+1} = 2 \\ \frac{(1-\chi)(1-q_{22})}{1-\chi+(2\chi-1)q_{22}}, & \text{if } n_t = 2, S_t = 2, S_{t+1} = 1 \\ \frac{\chi q_{22}}{1-\chi+(2\chi-1)q_{22}}, & \text{if } n_t = 2, S_t = 2, S_{t+1} = 2. \end{cases}
 \end{aligned} \tag{A-14}$$

Putting these two back into (A-13) gives a 4-state transition matrix

$$\begin{aligned}
 p(S_{t+1}, n_{t+1}|S_t, n_t, y_t, \Pi, \theta) &= \Pi'_B = \\
 \left[\begin{array}{cccc} \frac{\chi q_{11}(1-\chi+(2\chi-1)q_{11})}{1-\chi+(2\chi-1)q_{11}} & \frac{\chi q_{11}(\chi-(2\chi-1)q_{11})}{1-\chi+(2\chi-1)q_{11}} & \frac{(1-\chi)(1-q_{11})(\chi-(2\chi-1)q_{22})}{1-\chi+(2\chi-1)q_{11}} & \frac{(1-\chi)(1-q_{11})(1-\chi+(2\chi-1)q_{22})}{1-\chi+(2\chi-1)q_{11}} \\ \frac{(1-\chi)q_{11}(1-\chi+(2\chi-1)q_{11})}{\chi-(2\chi-1)q_{11}} & \frac{(1-\chi)q_{11}(\chi-(2\chi-1)q_{11})}{\chi-(2\chi-1)q_{11}} & \frac{\chi(1-q_{11})(\chi-(2\chi-1)q_{22})}{\chi-(2\chi-1)q_{11}} & \frac{\chi(1-q_{11})(1-\chi+(2\chi-1)q_{22})}{\chi-(2\chi-1)q_{11}} \\ \frac{\chi(1-q_{22})(1-\chi+(2\chi-1)q_{11})}{\chi-(2\chi-1)q_{22}} & \frac{\chi(1-q_{22})(\chi-(2\chi-1)q_{11})}{\chi-(2\chi-1)q_{22}} & \frac{(1-\chi)q_{22}(\chi-(2\chi-1)q_{22})}{\chi-(2\chi-1)q_{22}} & \frac{(1-\chi)q_{22}(1-\chi+(2\chi-1)q_{22})}{\chi-(2\chi-1)q_{22}} \\ \frac{(1-\chi)(1-q_{22})(1-\chi+(2\chi-1)q_{11})}{1-\chi+(2\chi-1)q_{22}} & \frac{(1-\chi)(1-q_{22})(\chi-(2\chi-1)q_{11})}{1-\chi+(2\chi-1)q_{22}} & \frac{\chi q_{22}(\chi-(2\chi-1)q_{22})}{1-\chi+(2\chi-1)q_{22}} & \frac{\chi q_{22}(1-\chi+(2\chi-1)q_{22})}{1-\chi+(2\chi-1)q_{22}} \end{array} \right].
 \end{aligned} \tag{A-15}$$

The rows and columns of the transition matrix correspond to $\kappa_t \in \{1, 2, 3, 4\}$ where

$$\kappa_t = \begin{cases} 1 & \text{if } S_t = 1, n_t = 1 \\ 2 & \text{if } S_t = 1, n_t = 2 \\ 3 & \text{if } S_t = 2, n_t = 1 \\ 4 & \text{if } S_t = 2, n_t = 2. \end{cases} \tag{A-16}$$

The rows are time t and columns are time $t + 1$ so that one can get conditional means in time t by pre-multiplying outcomes with this matrix .

C Hamilton Filter

Define α_t as the 4×1 vector with i^{th} element equal to one when $\kappa_t = i$ in and all other elements equal to zero (refer to A-16) . This implies that $E(\alpha_t|\alpha_{t-1}) = \Pi_B \alpha_{t-1}$ or

$$\alpha_t = \Pi_B \alpha_{t-1} + \xi_t \quad (\text{A-17})$$

where ξ_t is a disturbance vector uncorrelated with α_{t-1} . Note that the transition probabilities satisfy the condition $\sum_i \pi_{ij} = 1$ for $j = 1, \dots, 4$. The disturbance term ξ_t can take one of a possible set of 4^2 discrete values and so is not normally distributed.

Note that $p(S_{t+1}|S_t, n_t, \Pi, \theta) = \Psi \Pi_B \alpha_t$ where $\Psi = \begin{bmatrix} 1 & 1 & 0 & 0 \end{bmatrix}$. We define

$$z_t = \Phi(w_t), \quad \text{where} \quad w_t \sim N(\xi_t, \sigma_z^2) \quad (\text{A-18})$$

where

$$\xi_t = b_z + \Phi^{-1}(p(S_{t+1} = 1|S_t, n_t, \Pi, \theta)) = b_z + \Phi^{-1}(\Psi \Pi_B \alpha_t). \quad (\text{A-19})$$

Then,

$$p(z_t|S_t, n_t, y_t, \Pi, \theta) = f_w(\Phi^{-1}(z_t); \xi_t, \sigma_z^2) \times \left| \frac{1}{\phi(\Phi^{-1}(z_t))} \right| \quad (\text{A-20})$$

where $f_w(\cdot)$ is a density function of $\mathcal{N}(\xi_t, \sigma_z^2)$ and $\phi(\cdot)$ is a pdf of the standard normal distribution.²⁴

Define $x_t = [y_t, z_t]$ and $\mathcal{I}_t = x^t$. The Hamilton filter is an iterative algorithm for calculating the distribution of the state variable α_t .

$$\begin{aligned} \alpha_{t|t} &= E(\alpha_t|\mathcal{I}_t) \\ \alpha_{t|t-1} &= E(\alpha_t|\mathcal{I}_{t-1}) \end{aligned}$$

with the i^{th} element given by $Pr(\kappa_t = i|\mathcal{I}_t)$ and $Pr(\kappa_t = i|\mathcal{I}_{t-1})$, respectively. The

²⁴Note that $\Phi(\Phi^{-1}(z_t)) = z_t$, thus

$$\begin{aligned} \frac{\partial \Phi(\Phi^{-1}(z_t))}{\partial z_t} &= \phi(\Phi^{-1}(z_t)) \frac{\partial(\Phi^{-1}(z_t))}{\partial z_t} = 1 \\ \frac{\partial(\Phi^{-1}(z_t))}{\partial z_t} &= \frac{1}{\phi(\Phi^{-1}(z_t))}. \end{aligned}$$

Hamilton filter comprises two recursive equations: (1) the prediction equation, defining $\alpha_{t|t-1}$ and (2) the updating equation, defining $\alpha_{t|t}$.

Prediction Equation. The Hamilton filter prediction equation is

$$\alpha_{t|t-1} = \Pi_B \alpha_{t-1}. \quad (\text{A-21})$$

Updating Equation. The log-likelihood function of the observations x_t is given by

$$L = \sum_{t=1}^T \log p(x_t | \kappa_t, \mathcal{I}_{t-1}, \Pi, \theta) \quad (\text{A-22})$$

where

$$\begin{aligned} p(x_t | \kappa_t, \mathcal{I}_{t-1}) &= p(y_t | \kappa_t, \mathcal{I}_{t-1}, \Pi, \theta) p(z_t | y_t, \kappa_t, \mathcal{I}_{t-1}, \Pi, \theta) \\ &= N\left([\mu_1, \mu_1, \mu_2, \mu_2] \alpha_t, [\sigma_1^2, \sigma_1^2, \sigma_2^2, \sigma_2^2] \alpha_t\right) f_w(\Phi^{-1}(z_t); \xi_t, \sigma_z^2) \left| \frac{1}{\phi(\Phi^{-1}(z_t))} \right|. \end{aligned}$$

The ratio of the two represents the optimal inference on κ_t based on \mathcal{I}_t :

$$Pr(\kappa_t = i | \mathcal{I}_t, \Pi, \theta) = \frac{p(x_t, \kappa_t = i | \mathcal{I}_{t-1}, \Pi, \theta)}{p(x_t | \mathcal{I}_{t-1}, \Pi, \theta)}. \quad (\text{A-23})$$

Define v_t to be the $n \times 1$ vector with i^{th} element given by $p(x_t | \kappa_t = i, \mathcal{I}_{t-1}, \Pi, \theta)$. Then, the marginal distribution is

$$p(x_t | \mathcal{I}_{t-1}, \Pi, \theta) = v_t' \alpha_{t|t-1} \quad (\text{A-24})$$

and $p(x_t, \kappa_t = i | \mathcal{I}_{t-1}, \Pi, \theta)$ is the i^{th} element of the $n \times 1$ vector

$$v_t \odot \alpha_{t|t-1} \quad (\text{A-25})$$

where \odot is the element by element multiplication operator. Thus, equation (A-23) can be written as the (nonlinear) updating equation for $\alpha_{t|t}$

$$\alpha_{t|t} = \frac{v_t \odot \alpha_{t|t-1}}{v_t' \alpha_{t|t-1}}. \quad (\text{A-26})$$

D Parameter Learning (Without News)

Parameters. The joint prior over the mean μ_i and the variance σ_i^2 is Normal-Inverse-Gamma where

$$\begin{aligned} p(\sigma_i^2|y^t, S^t, \Pi) &= IG(\frac{v_{i,t}}{2}, \frac{K_{i,t}}{2}) \\ p(\mu_i|\sigma_i^2, y^t, S^t, \Pi) &= N(m_{i,t}, \sigma_i^2 C_{i,t}). \end{aligned} \quad (\text{A-27})$$

and since they are independent

$$\begin{aligned} p(\mu|\sigma^2, y^t, S^t, \Pi) &= p(\mu_i|\sigma^2, y^t, S^t, \Pi)p(\mu_j|\sigma^2, y^t, S^t, \Pi) \\ p(\sigma^2|y^t, S^t, \Pi) &= p(\sigma_i^2|y^t, S^t, \Pi)p(\sigma_j^2|y^t, S^t, \Pi). \end{aligned} \quad (\text{A-28})$$

These prior beliefs lead to posterior beliefs that are of the same form. The joint posterior distribution of the mean μ and the variance σ^2 can be factorized as

$$p(\mu, \sigma^2|y^{t+1}, S^{t+1}, \Pi) = p(\mu|\sigma^2, y^{t+1}, S^{t+1}, \Pi)p(\sigma^2|y^{t+1}, S^{t+1}, \Pi). \quad (\text{A-29})$$

Note that

$$\begin{aligned} p(\mu|\sigma^2, y^{t+1}, S^{t+1}, \Pi) &\propto p(y_{t+1}, S_{t+1}|\mu, \sigma^2, y^t, S^t, \Pi)p(\mu|\sigma^2, y^t, S^t, \Pi) \\ &= p(y_{t+1}|\mu, \sigma^2, y^t, S^{t+1}, \Pi)p(S_{t+1}|\mu, \sigma^2, y^t, S^t, \Pi)p(\mu|\sigma^2, y^t, S^t, \Pi) \end{aligned} \quad (\text{A-30})$$

$$\begin{aligned} p(\sigma^2|y^{t+1}, S^{t+1}, \Pi) &\propto p(y_{t+1}, S_{t+1}|\sigma^2, y^t, S^t, \Pi)p(\sigma^2|y^t, S^t, \Pi) \\ &= p(y_{t+1}|S_{t+1}, \sigma^2, y^t, S^t, \Pi)p(S_{t+1}|\sigma^2, y^t, S^t, \Pi)p(\sigma^2|y^t, S^t, \Pi) \end{aligned} \quad (\text{A-31})$$

Assume that $S_{t+1} = i$. We re-express (A-30) as

$$\begin{aligned}
p(\mu|\sigma^2, y^{t+1}, S^{t+1}) &\propto p(y_{t+1}|S_{t+1}, \mu, \sigma^2, y^t, S^t, \Pi)p(S_{t+1}|\mu, \sigma^2, y^t, S^t, \Pi)p(\mu|\sigma^2, y^t, S^t, \Pi) \\
&\propto p(y_{t+1}|S_{t+1}, \mu, \sigma^2, y^t, S^t, \Pi)p(\mu|\sigma^2, y^t, S^t, \Pi) \\
&= \left(\sum_{i=1}^2 \mathbb{I}_{\{S_{t+1}=i\}} \frac{1}{\sqrt{2\pi\sigma_i^2}} \exp \left\{ -\frac{1}{2\sigma_i^2} (y_{t+1} - \mu_i)^2 \right\} \right) \\
&\times \frac{1}{\sqrt{2\pi\sigma_i^2 C_{i,t}}} \exp \left\{ -\frac{(\mu_i - m_{i,t})^2}{2\sigma_i^2 C_{i,t}} \right\} \times \frac{1}{\sqrt{2\pi\sigma_j^2 C_{j,t}}} \exp \left\{ -\frac{(\mu_j - m_{j,t})^2}{2\sigma_j^2 C_{j,t}} \right\} \\
&\propto \frac{1}{\sqrt{2\pi(1 + \frac{1}{C_{i,t}})^{-1}\sigma_i^2}} \exp \left\{ -\frac{1}{2\sigma_i^2} \left(1 + \frac{1}{C_{i,t}}\right) \left(\mu_i - \frac{y_{t+1} + \frac{m_{i,t}}{C_{i,t}}}{1 + \frac{1}{C_{i,t}}}\right)^2 \right\} \\
&= N(m_{i,t+1}, C_{i,t+1}\sigma_i^2).
\end{aligned} \tag{A-32}$$

We can deduce that, $\forall i = \{1, 2\}$,

$$\begin{aligned}
C_{i,t+1} &= \left(\mathbb{I}_{\{S_{t+1}=i\}} + \frac{1}{C_{i,t}} \right)^{-1} \\
\frac{1}{C_{i,t+1}} &= \frac{1}{C_{i,t}} + \mathbb{I}_{\{S_{t+1}=i\}} \\
m_{i,t+1} &= \left(\mathbb{I}_{\{S_{t+1}=i\}} + \frac{1}{C_{i,t}} \right)^{-1} (\mathbb{I}_{\{S_{t+1}=i\}} y_{t+1} + \frac{m_{i,t}}{C_{i,t}}) \\
&= C_{i,t+1} (y_{t+1} \mathbb{I}_{\{S_{t+1}=i\}} + \frac{m_{i,t}}{C_{i,t}}) \\
\frac{m_{i,t+1}}{C_{i,t+1}} &= \frac{m_{i,t}}{C_{i,t}} + y_{t+1} \mathbb{I}_{\{S_{t+1}=i\}}.
\end{aligned} \tag{A-33}$$

Analogously for σ^2 ,

$$\begin{aligned}
p(\sigma^2|y^{t+1}, S^{t+1}, \Pi) &\propto p(y_{t+1}|\sigma^2, y^t, S^{t+1}, \Pi)p(S_{t+1}|\sigma^2, y^t, S^t, \Pi)p(\sigma^2|y^t, S^t, \Pi) \\
&\propto \left(\sum_{i=1}^2 \mathbb{I}_{\{S_{t+1}=i\}} \frac{1}{\sqrt{2\pi(C_{i,t} + 1)\sigma_i^2}} \exp \left\{ -\frac{1}{2\sigma_i^2} \frac{(y_{t+1} - m_{i,t})^2}{(C_{i,t} + 1)} \right\} \right) \\
&\times \frac{\left(\frac{K_{i,t}}{2}\right)^{\left(\frac{v_{i,t}}{2}\right)}}{\Gamma\left(\frac{v_{i,t}}{2}\right)} (\sigma_i^2)^{-\frac{v_{i,t}}{2}-1} e^{-\frac{K_{j,t}}{2\sigma_j^2}} \times \frac{\left(\frac{K_{j,t}}{2}\right)^{\left(\frac{v_{j,t}}{2}\right)}}{\Gamma\left(\frac{v_{j,t}}{2}\right)} (\sigma_j^2)^{-\frac{v_{j,t}}{2}-1} e^{-\frac{K_{j,t}}{2\sigma_j^2}} \\
&\propto (\sigma_i^2)^{-\frac{v_{i,t}+1}{2}-1} \exp \left\{ -\frac{1}{\sigma_i^2} \frac{\left(K_{i,t} + \frac{(y_{t+1} - m_{i,t})^2}{(C_{i,t} + 1)}\right)}{2} \right\}
\end{aligned} \tag{A-34}$$

from which we can deduce that

$$\begin{aligned} v_{i,t+1} &= v_{i,t} + \mathbb{I}_{\{S_{t+1}=i\}} \\ K_{i,t+1} &= K_{i,t} + \frac{(y_{t+1} - m_{i,t})^2}{(C_{i,t} + 1)} \mathbb{I}_{\{S_{t+1}=i\}}. \end{aligned} \quad (\text{A-35})$$

Transition Probabilities. At $t = 0$, the agent is given an initial (potentially truncated) Beta-distributed prior over each of these parameters and thereafter updates beliefs sequentially upon observing the time-series of realized regimes, S_t . The prior Beta-distribution coupled with the realization of regimes leads to a conjugate prior and so posterior beliefs are also Beta-distributed. The probability density function of the Beta-distribution is

$$p(\pi|a, b) = \frac{\pi^{a-1}(1-\pi)^{b-1}}{B(a, b)}, \quad (\text{A-36})$$

where $B(a, b)$ is the Beta function (a normalization constant). The parameters a and b govern the shape of the distribution. The expected value is

$$E(\pi|a, b) = \frac{a}{a+b}. \quad (\text{A-37})$$

The standard Bayes rule shows that the updating equations count the number of times state i has been followed by state i versus the number of times state i has been followed by state j . Given this sequential updating, we let the a and b parameters have a subscript for the relevant state (1 or 2) and a time subscript

$$\begin{aligned} a_{i,t} &= a_{i,0} + \# \text{ (state } i \text{ has been followed by state } i), \\ b_{i,t} &= b_{i,0} + \# \text{ (state } i \text{ has been followed by state } j). \end{aligned} \quad (\text{A-38})$$

The law of motions for $a_{i,t}$ and $b_{i,t}$ are

$$\begin{aligned} a_{i,t+1} &= a_{i,t} + \mathbb{I}_{\{S_{t+1}=i\}} \mathbb{I}_{\{S_t=i\}} \\ b_{i,t+1} &= b_{i,t} + (1 - \mathbb{I}_{\{S_{t+1}=i\}}) \mathbb{I}_{\{S_t=i\}}. \end{aligned} \quad (\text{A-39})$$

We can deduce that posterior distribution of Π is

$$p(\Pi|y^{t+1}, S^{t+1}, \theta) = B(a_{1,t+1}, b_{1,t+1})B(a_{2,t+1}, b_{2,t+1}). \quad (\text{A-40})$$

E Particle Learning

We collect two observations in

$$x_t = [y_t, z_t]$$

and the model parameters are collected in

$$\theta = (\mu_1, \mu_2, \sigma_1^2, \sigma_2^2), \quad \Pi = (q_{11}, q_{22}), \quad \Lambda = (\chi, \sigma_z^2).$$

Denote sufficient statistics for θ , Π , and Λ by $F_{\theta,t}$, $F_{\Pi,t}$, and $F_{\Lambda,t}$ respectively. Specifically,

$$F_{\theta,t} = \{m_{i,t}, C_{i,t}, v_{i,t}, K_{i,t}\}_{i=1}^2, \quad F_{\Pi,t} = \{a_{i,t}, b_{i,t}\}_{i=1}^2, \quad F_{\Lambda,t} = \{a_{z,t}, b_{z,t}, v_{z,t}, K_{z,t}\}. \quad (\text{A-41})$$

Sufficient statistics imply that the full posterior distribution of the parameters conditional on the entire history of latent states and data takes a known functional form conditional on a vector of sufficient statistics:

$$p(\theta, \Pi, \Lambda | x^t, \kappa^t) = p(\theta, \Pi, \Lambda | F_{\theta,t}, F_{\Pi,t}, F_{\Lambda,t}) = p(\theta | F_{\theta,t})p(\Pi | F_{\Pi,t})p(\Lambda | F_{\Lambda,t}). \quad (\text{A-42})$$

Ultimately, we are interested in

$$p(\theta, \Pi, \Lambda, \kappa^t | x^t) = p(\theta, \Pi, \Lambda | \kappa^t, x^t)p(\kappa^t | x^t). \quad (\text{A-43})$$

The idea of particle learning is to sample from $p(\theta, \Pi, \Lambda, F_{\theta,t}, F_{\Pi,t}, F_{\Lambda,t}, \kappa^t | x^t)$ than from $p(\theta, \Pi, \Lambda, \kappa^t | x^t)$.

$$p(\theta, \Pi, \Lambda, F_{\theta,t}, F_{\Pi,t}, F_{\Lambda,t}, \kappa^t | x^t) = \underbrace{p(\theta, \Pi, \Lambda | F_{\theta,t}, F_{\Pi,t}, F_{\Lambda,t})}_{(4) \text{ Drawing Parameters}} \times \underbrace{p(F_{\theta,t}, F_{\Pi,t}, F_{\Lambda,t}, \kappa^t | x^t)}_{\substack{\text{Propagating (2) State,} \\ \text{(3) Sufficient Statistics}}}. \quad (\text{A-44})$$

The particle learning algorithm can be described through the following steps.

E.1 Algorithm

Assume at time t , we have particles $\left\{ \kappa_t^{(k)}, \theta^{(k)}, \Pi^{(k)}, \Lambda^{(k)}, F_{\theta,t}^{(k)}, F_{\Pi,t}^{(k)}, F_{\Lambda,t}^{(k)} \right\}_{k=1}^N$.

1. Resample Particles:

Resample $\left\{ \kappa_t^{(k)}, \theta^{(k)}, \Pi^{(k)}, \Lambda^{(k)}, F_{\theta,t}^{(k)}, F_{\Pi,t}^{(k)}, F_{\Lambda,t}^{(k)} \right\}$ with weights $w_t^{(k)}$,

$$\begin{aligned} w_{t+1}^{(k)} &\propto \sum_{i=1}^2 p \left(x_{t+1} | \kappa_{t+1} = i, \left\{ \kappa_t^{(k)}, \theta^{(k)}, \Pi^{(k)}, \Lambda^{(k)}, F_{\theta,t}^{(k)}, F_{\Pi,t}^{(k)}, F_{\Lambda,t}^{(k)} \right\} \right) \\ &\quad \times p \left(\kappa_{t+1} = i | \left\{ \kappa_t^{(k)}, \theta^{(k)}, \Pi^{(k)}, \Lambda^{(k)}, F_{\theta,t}^{(k)}, F_{\Pi,t}^{(k)}, F_{\Lambda,t}^{(k)} \right\} \right). \end{aligned} \quad (\text{A-45})$$

Denote them by $\left\{ \tilde{\kappa}_t^{(k)}, \tilde{\theta}^{(k)}, \tilde{\Pi}^{(k)}, \tilde{\Lambda}^{(k)}, \tilde{F}_{\theta,t}^{(k)}, \tilde{F}_{\Pi,t}^{(k)}, \tilde{F}_{\Lambda,t}^{(k)} \right\}_{k=1}^N$.

2. Propagate State:

$$\kappa_{t+1}^{(k)} \sim p \left(\kappa_{t+1} | x_{t+1}, \left\{ \tilde{\kappa}_t^{(k)}, \tilde{\theta}^{(k)}, \tilde{\Pi}^{(k)}, \tilde{\Lambda}^{(k)}, \tilde{F}_{\theta,t}^{(k)}, \tilde{F}_{\Pi,t}^{(k)}, \tilde{F}_{\chi,t}^{(k)} \right\} \right).$$

3. Propagate Sufficient Statistics:

$$(a) \quad F_{\theta,t+1} \sim \mathcal{F}(\tilde{F}_{\theta,t}^{(k)}, S_{t+1}^{(k)}, x_{t+1}).$$

$$\begin{aligned} \frac{m_{i,t+1}^{(k)}}{C_{i,t+1}^{(k)}} &= \frac{\tilde{m}_{i,t}^{(k)}}{\tilde{C}_{i,t}^{(k)}} + y_{t+1} \mathbb{I}_{\{S_{t+1}^{(k)}=i\}} \\ \frac{1}{C_{i,t+1}^{(k)}} &= \frac{1}{\tilde{C}_{i,t}^{(k)}} + \mathbb{I}_{\{S_{t+1}^{(k)}=i\}} \\ v_{i,t+1}^{(k)} &= \tilde{v}_{i,t}^{(k)} + \mathbb{I}_{\{S_{t+1}^{(k)}=i\}} \\ K_{i,t+1}^{(k)} &= \tilde{K}_{i,t}^{(k)} + \frac{(y_{t+1} - \tilde{m}_{i,t}^{(k)})^2}{(\tilde{C}_{i,t}^{(k)} + 1)} \mathbb{I}_{\{S_{t+1}^{(k)}=i\}}. \end{aligned} \quad (\text{A-46})$$

$$(b) \quad F_{\Pi,t+1} \sim \mathcal{F}(\tilde{F}_{\Pi,t}^{(k)}, S_{t+1}^{(k)}, x_{t+1}).$$

$$\begin{aligned} a_{i,t+1}^{(k)} &= \tilde{a}_{i,t}^{(k)} + \mathbb{I}_{\{S_{t+1}^{(k)}=i\}} \mathbb{I}_{\{S_t^{(k)}=i\}} \\ b_{i,t+1}^{(k)} &= \tilde{b}_{i,t}^{(k)} + (1 - \mathbb{I}_{\{S_{t+1}^{(k)}=i\}}) \mathbb{I}_{\{S_t^{(k)}=i\}}. \end{aligned} \quad (\text{A-47})$$

$$(c) \ F_{\Lambda,t+1} \sim \mathcal{F}(\tilde{F}_{\Lambda,t}^{(k)}, S_{t+1}^{(k)}, n_{t+1}^{(k)}, x_{t+1}).$$

$$\begin{aligned} a_{z,t+1}^{(k)} &= \tilde{a}_{z,t}^{(k)} + \mathbb{I}_{\{S_{t+1}^{(k)}=i\}} \mathbb{I}_{\{n_t^{(k)}=i\}} \\ b_{z,t+1}^{(k)} &= \tilde{b}_{z,t}^{(k)} + (1 - \mathbb{I}_{\{S_{t+1}^{(k)}=i\}}) \mathbb{I}_{\{n_t^{(k)}=i\}} \\ v_{z,t+1}^{(k)} &= \tilde{v}_{z,t}^{(k)} + 1 \\ K_{z,t+1}^{(k)} &= \tilde{K}_{z,t}^{(k)} + (\Phi^{-1}(z_t) - \tilde{\xi}_t)^2 \end{aligned} \tag{A-48}$$

where $\tilde{\xi}_t$ is provided in (A-19).

Note that \mathcal{F} s are analytically known.

4. Draw Parameters:

$$(a) \ \theta^{(k)} \sim p(\theta | F_{\theta,t+1}).$$

$$\begin{aligned} \sigma_i^{2,(k)} &\sim IG\left(\frac{v_{i,t+1}^{(k)}}{2}, \frac{K_{i,t+1}^{(k)}}{2}\right) \\ \mu_i^{(k)} &\sim N(m_{i,t+1}^{(k)}, \sigma_i^{2,(k)} C_{i,t+1}^{(k)}). \end{aligned} \tag{A-49}$$

$$(b) \ \Pi^{(k)} \sim p(\Pi | F_{\Pi,t+1}).$$

$$\begin{aligned} q_{11}^{(k)} &\sim B(a_{1,t+1}^{(k)}, b_{1,t+1}^{(k)}) \\ q_{22}^{(k)} &\sim B(a_{2,t+1}^{(k)}, b_{2,t+1}^{(k)}). \end{aligned} \tag{A-50}$$

$$(c) \ \Lambda^{(k)} \sim p(\Lambda | F_{\Lambda,t+1}).$$

$$\chi^{(k)} \sim B(a_{z,t+1}^{(k)}, b_{z,t+1}^{(k)}) \tag{A-51}$$

$$\sigma_z^{2,(k)} \sim IG\left(\frac{v_{z,t+1}^{(k)}}{2}, \frac{K_{z,t+1}^{(k)}}{2}\right). \tag{A-52}$$

To initialize the algorithm, we provide the priors in Table A-1. The length of the prior training sample (prior precision), T^{prior} , is set to 10 years.

Table A-1: Priors

| Parameter | 5% | 50% | 95% | Sufficient Statistics | Distribution |
|--------------|------|------|------|-----------------------|------------------------------------|
| μ_1 | -1.0 | 1.0 | 3.0 | $m_{1,0}, C_{1,0}$ | $N(1, 0.5), IG(1, 2/3)$ |
| σ_1^2 | 0.12 | 0.40 | 1.50 | $v_{1,0}, K_{1,0}$ | $G(5, 5), G(5, 2)$ |
| μ_2 | -2.0 | 0.0 | 2.0 | $m_{2,0}, C_{2,0}$ | $N(0, 0.5), IG(1, 2/3)$ |
| σ_2^2 | 0.12 | 0.40 | 1.50 | $v_{2,0}, K_{2,0}$ | $G(5, 5), G(5, 2)$ |
| q_{11} | 0.64 | 0.80 | 0.93 | $a_{1,0}, b_{1,0}$ | $Mult(T^{\text{prior}}, 0.8, 0.2)$ |
| q_{22} | 0.64 | 0.80 | 0.93 | $a_{2,0}, b_{2,0}$ | $Mult(T^{\text{prior}}, 0.8, 0.2)$ |
| χ | 0.64 | 0.80 | 0.93 | $a_{z,0}, b_{z,0}$ | $Mult(T^{\text{prior}}, 0.8, 0.2)$ |
| σ_z^2 | 0.06 | 0.24 | 0.96 | $v_{z,0}, K_{z,0}$ | $G(5, 5), G(3, 2)$ |

Notes: N , G , IG , $Mult$ are normal distribution, gamma distribution, inverse gamma distribution, multinomial distribution, respectively.

F Asset Pricing Solution

F.1 Sufficient statistics

In our asset pricing model, we assume that agents' information sets at time t are $I_t = \{\kappa^t, y^t, \theta\}$ and they rationally learn the transition probabilities Π using observed data. To conserve notation, we now add to the parameter vector θ parameters governing the prior beliefs about Π as well as preference and dividend process parameters from the asset pricing model. We follow Collin-Dufresne, Johannes, and Lochstoer (2016)) in mapping the sufficient statistics of the Bayesian learning problem in Appendix A to an alternative set of statistics which yield a more convenient solution method. More specifically, we map $\{a_{1,t}, b_{1,t}, a_{2,t}, b_{2,t}\}$ to $X_t \equiv \{\lambda_{1,t}, \tau_{1,t}, \lambda_{2,t}, \tau_{2,t}\}$ as follows:

$$\begin{aligned}
\tau_{1,t} &= a_{1,t} - a_{1,0} + b_{1,t} - b_{1,0}, \\
\lambda_{1,t} &= \frac{a_{1,t}}{a_{1,t} + b_{1,t}}, \\
\tau_{2,t} &= a_{2,t} - a_{2,0} + b_{2,t} - b_{2,0}, \\
\lambda_{2,t} &= \frac{a_{2,t}}{a_{2,t} + b_{2,t}}.
\end{aligned}$$

Note that the expressions for the posterior estimates of Π given in Appendix A can be rewritten in terms of $\{\lambda_{1,t}, \tau_{1,t}, \lambda_{2,t}, \tau_{2,t}, \theta\}$. Further, note that X_t follows a process that

depends only on its own lag as well as $\{\kappa_t, \kappa_{t-1}\}$:

$$\begin{aligned}\lambda_{1,t} &= \lambda_1(\kappa_t, \kappa_{t-1}, X_{t-1}, \theta) = \lambda_{1,t-1} + \frac{\mathbb{I}\{S_t = 1\} - \lambda_{1,t-1}}{a_{1,0} + b_{1,0} + \tau_{1,t-1} + 1}, \\ \tau_{1,t} &= \tau_1(\kappa_t, \kappa_{t-1}, X_{t-1}, \theta) = \tau_{1,t-1} + \mathbb{I}\{S_{t-1} = 1\}, \\ \lambda_{2,t} &= \lambda_2(\kappa_t, \kappa_{t-1}, X_{t-1}, \theta) = \lambda_{2,t-1} + \frac{\mathbb{I}\{S_t = 2\} - \lambda_{2,t-1}}{a_{2,0} + b_{2,0} + \tau_{2,t-1} + 1}, \\ \tau_{2,t} &= \tau_2(\kappa_t, \kappa_{t-1}, X_{t-1}, \theta) = \tau_{2,t-1} + \mathbb{I}\{S_{t-1} = 2\}.\end{aligned}\tag{A-53}$$

Lastly, this set of sufficient statistics simplifies the solution method because now only two of the sufficient statistics grow without bound ($\tau_{1,t}$ and $\tau_{2,t}$) while $\lambda_{1,t}, \lambda_{2,t} \in [0, 1]$.

For the solution below, agents' belief about the probability of κ_{t+1} conditional on I_t is given by:

$$\begin{aligned}p(\kappa_{t+1}|I_t) &= p(\kappa_{t+1}|\kappa_t, y_t, X_t, \theta) \\ &= \int p(\kappa_{t+1}|\kappa_t, X_t, y_t, \Pi, \theta)p(\Pi|\kappa_t, y_t, X_t, \theta)d\Pi\end{aligned}$$

where $p(\kappa_{t+1}|\kappa_t, X_t, y_t, \Pi, \theta) = \Pi_B^T$ as defined in (A-15) and $p(\Pi|\kappa_t, y_t, X_t, \theta) = p(\Pi|n_t, S^t, \theta)$ as given in (A-12). Solving this integration yields:

$$\Pi_{B,t}^T \equiv p(\kappa_{t+1}|\kappa_t, X_t, y_t, \Pi, \theta) = \tag{A-54}$$

$$\begin{bmatrix} \frac{\lambda_1 \chi [\chi \lambda'_1 + (1-\chi)(1-\lambda'_1)]}{\lambda_1 \chi + (1-\lambda_1)(1-\chi)} & \frac{\lambda_1 \chi [(1-\chi)\lambda'_1 + \chi(1-\lambda'_1)]}{\lambda_1 \chi + (1-\lambda_1)(1-\chi)} & \frac{(1-\lambda_1)(1-\chi)[\chi(1-\lambda'_2) + (1-\chi)\lambda'_2]}{\lambda_1 \chi + (1-\lambda_1)(1-\chi)} & \frac{(1-\lambda_1)(1-\chi)[(1-\chi)(1-\lambda'_2) + \chi\lambda'_2]}{\lambda_1 \chi + (1-\lambda_1)(1-\chi)} \\ \frac{\lambda_1(1-\chi)[\chi\lambda'_1 + (1-\chi)(1-\lambda'_1)]}{\lambda_1(1-\chi) + (1-\lambda_1)\chi} & \frac{\lambda_1(1-\chi)[(1-\chi)\lambda'_1 + \chi(1-\lambda'_1)]}{\lambda_1(1-\chi) + (1-\lambda_1)\chi} & \frac{(1-\lambda_1)\chi[\chi(1-\lambda'_2) + (1-\chi)\lambda'_2]}{\lambda_1 \chi + (1-\lambda_1)(1-\chi)} & \frac{(1-\lambda_1)\chi[(1-\chi)(1-\lambda'_2) + \chi\lambda'_2]}{\lambda_1 \chi + (1-\lambda_1)(1-\chi)} \\ \frac{(1-\lambda_2)\chi[\chi\lambda'_1 + (1-\chi)(1-\lambda'_1)]}{(1-\lambda_2)\chi + \lambda_2(1-\chi)} & \frac{(1-\lambda_2)\chi[(1-\chi)\lambda'_1 + \chi(1-\lambda'_1)]}{(1-\lambda_2)\chi + \lambda_2(1-\chi)} & \frac{\lambda_2(1-\chi)[\chi(1-\lambda'_2) + (1-\chi)\lambda'_2]}{(1-\lambda_2)\chi + \lambda_2(1-\chi)} & \frac{\lambda_2(1-\chi)[(1-\chi)(1-\lambda'_2) + \chi\lambda'_2]}{(1-\lambda_2)\chi + \lambda_2(1-\chi)} \\ \frac{(1-\lambda_2)(1-\chi)[\chi\lambda'_1 + (1-\chi)(1-\lambda'_1)]}{(1-\lambda_2)(1-\chi) + \lambda_2\chi} & \frac{(1-\lambda_2)(1-\chi)[(1-\chi)\lambda'_1 + \chi(1-\lambda'_1)]}{(1-\lambda_2)(1-\chi) + \lambda_2\chi} & \frac{\lambda_2\chi[\chi(1-\lambda'_2) + (1-\chi)\lambda'_2]}{(1-\lambda_2)(1-\chi) + \lambda_2\chi} & \frac{\lambda_2\chi[(1-\chi)(1-\lambda'_2) + \chi\lambda'_2]}{(1-\lambda_2)(1-\chi) + \lambda_2\chi} \end{bmatrix},$$

where we use the short-hand notation $\lambda_i \equiv \lambda_{i,t}$ and $\lambda'_i \equiv \lambda_{i,t+1} = \lambda_i(\kappa_{t+1}, \kappa_t, X_t, \theta)$ for $i \in \{1, 2\}$. Note that in this section, the superscript T will be used to denote matrix transposition while $'$ will be used to denote next-period variables.

F.2 Wealth-consumption and price-dividend ratios

Agents have Epstein-Zin preferences given by

$$V_t = \left\{ (1 - \beta) C_t^{1-\frac{1}{\psi}} + \beta [E_t V_{t+1}^{1-\gamma}]^{\frac{1-\frac{1}{\psi}}{1-\gamma}} \right\}^{\frac{1}{1-\frac{1}{\psi}}}.$$

The consumption process is governed by the exogenous process for output as follows:

$$\Delta c_t = \Delta y_t = \mu_{s_t} + \sigma_{s_t} \varepsilon_t.$$

Lastly, we assume that the dividend process is given by,

$$\Delta d_{t+1} = \bar{\mu} + \rho (\Delta c_{t+1} - \bar{\mu}) + \sigma_d \eta_{t+1}.$$

The solution for the wealth-consumption ratio in this setting is

$$\begin{aligned} PC_t^\alpha &= E[\beta^\alpha e^{(1-\gamma)\Delta c_{t+1}} (PC_{t+1} + 1)^\alpha | I_t] \\ &= E[\beta^\alpha E[e^{(1-\gamma)\Delta c_{t+1}} | I_t, S_{t+1}] (PC_{t+1} + 1)^\alpha | I_t] \\ &= E[\beta^\alpha e^{(1-\gamma)\tilde{\mu}_{\kappa_{t+1}} + \frac{1}{2}(1-\gamma)^2 \tilde{\sigma}_{\kappa_{t+1}}^2} (PC_{t+1} + 1)^\alpha | I_t], \end{aligned}$$

where $\alpha \equiv \frac{1-\gamma}{1-1/\psi}$ and

$$\begin{aligned} \tilde{\mu}_1 &= \tilde{\mu}_2 = \mu_1, \quad \tilde{\mu}_3 = \tilde{\mu}_4 = \mu_2, \\ \tilde{\sigma}_1 &= \tilde{\sigma}_2 = \mu_1, \quad \tilde{\sigma}_3 = \tilde{\sigma}_4 = \mu_2. \end{aligned}$$

Similarly, the price-dividend ratio is

$$PD_t = E \left[\beta^\alpha e^{(\rho-\gamma)\tilde{\mu}_{\kappa_{t+1}} + \frac{1}{2}(\rho-\gamma)^2 \tilde{\sigma}_{\kappa_{t+1}}^2 + (1-\rho)\bar{\mu}(q_{11}, q_{22})} \left(\frac{PC_{t+1} + 1}{PC_t} \right)^{\alpha-1} (PD_{t+1} + 1) \middle| I_t \right].$$

where $\bar{\mu}(q_{11}, q_{22})$ is the long-run mean of consumption growth as a function of $\{q_{11}, q_{22}\}$.

Since the exogenous states are Markov and the sufficient statistics of the Bayesian learning problem satisfy $X_{t+1} = F(S_{t+1}, S_t, X_t)$ for a function F that summarizes (A-53), the equilibrium wealth-consumption and price-dividend ratios can be written as functions of state variables and known parameters $\{\kappa_t, X_t, \theta\}$ that satisfies the following

recursions:

$$PC(\kappa_t, X_t, \theta)^\alpha = E \left[\beta^\alpha e^{(1-\gamma)\tilde{\mu}_{\kappa_{t+1}} + \frac{1}{2}(1-\gamma)^2 \tilde{\sigma}_{\kappa_{t+1}}^2} (PC(\kappa_{t+1}, X_{t+1}, \theta) + 1)^\alpha | I_t \right],$$

$$\begin{aligned} PD(\kappa_t, X_t, \theta) &= E \left[\beta^\alpha e^{(\rho-\gamma)\tilde{\mu}_{\kappa_{t+1}} + \frac{1}{2}(\rho-\gamma)^2 \tilde{\sigma}_{\kappa_{t+1}}^2 + (1-\rho)\tilde{\mu}(q_{11}, q_{22})} \right. \\ &\quad \times \left. \left(\frac{PC(\kappa_{t+1}, X_{t+1}, \theta) + 1}{PC(\kappa_t, X_t, \theta)} \right)^{\alpha-1} (PD(\kappa_{t+1}, X_{t+1}, \theta) + 1) \middle| I_t \right]. \end{aligned}$$

We follow Collin-Dufresne, Johannes, and Lochstoer (2016)) in solving this recursion by using the property that beliefs about $\{q_{11}, q_{22}\}$ converge to the true values under Bayesian learning as $\{\tau_{1,t}, \tau_{2,t}\}$ grow. This allows us to iterate backwards from the known parameters solution. Details on this procedure are provided below:

F.3 Full information case (both q_{11}, q_{22} known)

Despite no impact of news on parameter learning in this case, n_t still serves as a signal about S_{t+1} . The relevant state transition matrix is the one given in (A-15). In this case, we solve for the equilibrium wealth-consumption and price-dividend ratios on a 3-dimensional grid of values for $\{\kappa, q_{11}, q_{22}\}$.

F.3.1 Wealth-consumption ratio

The equilibrium condition for the wealth-consumption ratio when $\{q_{11}, q_{22}\}$ are known is

$$\mathbf{PC}^{\circ\alpha} = \Pi_B^T \left(\beta^\alpha e^{(1-\gamma)\tilde{\mu}' + \frac{1}{2}(1-\gamma)^2 (\tilde{\sigma}')^{\circ 2}} \circ (\mathbf{PC}' + 1)^{\circ\alpha} \right),$$

where bolded variables now denote 4×1 vectors indexed by κ and dependence on $\{\Pi, \theta\}$ is suppressed for brevity. The symbol \circ is used to denote element-wise multiplication and exponentiation. For fixed values of $\{\Pi, \theta\}$, this is simply a system of 4 nonlinear equations which can be solved numerically.

F.3.2 Price-dividend ratio

Similarly, the price-dividend ratio can be obtained by solving the following system of equations:

$$\mathbf{PD} = \Pi_B^T \left(\beta^\alpha e^{(\rho-\gamma)\tilde{\mu}' + \frac{1}{2}(\rho-\gamma)^2(\tilde{\sigma}')^2 + (1-\rho)\tilde{\mu}} \circ ((\mathbf{PC}' + 1) \oslash \mathbf{PC})^{\circ(\alpha-1)} \circ (\mathbf{PD}' + 1) \right).$$

where \oslash denotes element-wise division.

F.4 Case with q_{ii} known and q_{jj} unknown

In this case, we need to carry a subset of the sufficient statistics $X_{j,t} \equiv \{\lambda_{j,t}, \tau_{j,t}\}$. The relevant state transition matrix is denoted by $\Pi_{B,t,ii}^T \equiv p(\kappa_{t+1} | \kappa_t, X_{j,t}, y_t, q_{ii}, \theta)$. One can show that this matrix is equal to (A-54) with the substitution $\lambda_i = q_{ii}$ in all time periods. For both sets of $\{i, j\}$, we solve for the equilibrium wealth-consumption and price-dividend ratios on a 4-dimensional grid of values for $\{\kappa, \lambda_j, \tau_j, q_{ii}\}$ where $\tau_{j,t}$ is truncated at a large value $\tau_{j,T}$.

F.4.1 Wealth-consumption ratio

Now, the wealth-consumption ratio is no longer stationary since $\tau_{j,t}$ grows without bound. It must satisfy the recursion

$$PC(\kappa_t, X_{j,t}, q_{ii}, \theta)^\alpha = E \left[\beta^\alpha e^{(1-\gamma)\tilde{\mu}_{\kappa_{t+1}} + \frac{1}{2}(1-\gamma)^2\tilde{\sigma}_{\kappa_{t+1}}^2} (PC(\kappa_{t+1}, X_{j,t+1}, q_{ii}, \theta) + 1)^\alpha | I_t \right].$$

To obtain the PC solution for a given q_{ii} , we start with the approximation that $PC(\kappa_T, X_{j,T}, q_{ii}, \theta) = PC(\kappa_T, \Pi, \theta)$ for some large $\tau_{j,T}$ since this relationship becomes exact as $\tau_{j,T} \rightarrow \infty$. We then iterate backwards by repeating the following two steps:

1. If $S_t = j$, $\lambda_{j,t+1}$ and $\tau_{j,t+1}$ will update as above for both $S_{t+1} = 1$ and $S_{t+1} = 2$ and any observation n_t would be informative so the values of PC for κ_t such that $S_t = j$ are a function of the values of PC with τ_j incremented by one. That is,

we iterate τ_j backwards one step as follows:

$$\begin{bmatrix} PC(\kappa_t = 2j - 1, \lambda_{j,t}, \tau_{j,t})^\alpha \\ PC(\kappa_t = 2j, \lambda_{j,t}, \tau_{j,t})^\alpha \end{bmatrix} = \beta^\alpha \Pi_{B,t,ii,[2j-1:2j]}^T \times \left(e^{(1-\gamma)\tilde{\mu}' + \frac{1}{2}(1-\gamma)^2(\tilde{\sigma}')^2} \circ \left(\begin{bmatrix} PC(\kappa_t = 1, \lambda_{j,t+1}, \tau_{j,t} + 1) \\ PC(\kappa_t = 2, \lambda_{j,t+1}, \tau_{j,t} + 1) \\ PC(\kappa_t = 3, \lambda_{j,t+1}, \tau_{j,t} + 1) \\ PC(\kappa_t = 4, \lambda_{j,t+1}, \tau_{j,t} + 1) \end{bmatrix} + 1 \right)^{\circ\alpha} \right),$$

where we use the fact that $\kappa_t = 2(S_t - 1) + n_t$ and $\Pi_{B,t,ii,[2j-1:2j]}^T$ is the 2×4 submatrix formed by rows $2j - 1$ and $2j$ of matrix $\Pi_{B,t,ii}^T$. The dependence on $\{q_{ii}, \theta\}$ is suppressed here for brevity.

2. If $S_t = i$, nothing can be learned about q_{jj} in the next period regardless of the value of S_{t+1} or n_t . In other words, $\lambda_{j,t+1} = \lambda_{j,t}$ and $\tau_{j,t+1} = \tau_{j,t}$ for $S_t = i$. Thus, given the values from the LHS of the previous step, we can directly solve for PC for the remaining values of κ_t using this system of equations:

$$\begin{bmatrix} PC(\kappa_t = 2i - 1, \lambda_{j,t}, \tau_{j,t})^\alpha \\ PC(\kappa_t = 2i, \lambda_{j,t}, \tau_{j,t})^\alpha \end{bmatrix} = \beta^\alpha \Pi_{B,t,ii,[2i-1:2i]}^T \left(e^{(1-\gamma)\tilde{\mu}' + \frac{1}{2}(1-\gamma)^2(\tilde{\sigma}')^2} \circ (\mathbf{PC}' + 1)^{\circ\alpha} \right),$$

where \mathbf{PC}' is formed by stacking

$$\begin{bmatrix} PC(\kappa_t = 2i - 1, \lambda_{j,t}, \tau_{j,t}) \\ PC(\kappa_t = 2i, \lambda_{j,t}, \tau_{j,t}) \end{bmatrix}, \quad \begin{bmatrix} PC(\kappa_t = 2j - 1, \lambda_{j,t}, \tau_{j,t}) \\ PC(\kappa_t = 2j, \lambda_{j,t}, \tau_{j,t}) \end{bmatrix}$$

appropriately given the values of i and j .

F.4.2 Price-dividend ratio

Once we have the solution for PC , the solution for the price-dividend ratio proceeds analogously based on the recursion

$$\begin{aligned} PD(\kappa_t, X_{j,t}, q_{ii}, \theta) &= E \left[\beta^\alpha e^{(\rho-\gamma)\tilde{\mu}_{\kappa_{t+1}} + \frac{1}{2}(\rho-\gamma)^2\tilde{\sigma}_{\kappa_{t+1}}^2 + (1-\rho)\tilde{\mu}(q_{ii}, q_{jj})} \right. \\ &\quad \times \left(\frac{PC(\kappa_{t+1}, X_{j,t+1}, q_{ii}, \theta) + 1}{PC(\kappa_t, X_{j,t+1}, q_{ii}, \theta)} \right)^{\alpha-1} (PD(\kappa_{t+1}, X_{j,t+1}, q_{ii}, \theta) + 1) \Big| I_t \Big]. \end{aligned}$$

We start with an analogous approximation that $PD(\kappa_T, X_{j,T}, q_{ii}, \theta) = PD(\kappa_T, \Pi, \theta)$ for some large $\tau_{j,T}$ and then iterate backwards by repeating the same two steps:

1. If $S_t = j$, we again iterate τ_j backwards one step as follows:

$$\begin{aligned} & \begin{bmatrix} PD(\kappa_t = 2j - 1, \lambda_{j,t}, \tau_{j,t}) \\ PD(\kappa_t = 2j, \lambda_{j,t}, \tau_{j,t}) \end{bmatrix} \\ = & \beta^\alpha \Pi_{B,t,ii,[2j-1:2j]}^T \times \left(e^{(\rho-\gamma)\tilde{\mu}' + \frac{1}{2}(\rho-\gamma)^2(\tilde{\sigma}')^2 + (1-\rho)\bar{\mu}(q_{ii}, \hat{q}_{jj})} \right. \\ & \left. \circ ((\mathbf{PC}' + 1) \oslash \mathbf{PC})^{\circ(\alpha-1)} \circ \left(\begin{bmatrix} PD(\kappa_t = 1, \lambda_{j,t+1}, \tau_{j,t} + 1) \\ PD(\kappa_t = 2, \lambda_{j,t+1}, \tau_{j,t} + 1) \\ PD(\kappa_t = 3, \lambda_{j,t+1}, \tau_{j,t} + 1) \\ PD(\kappa_t = 4, \lambda_{j,t+1}, \tau_{j,t} + 1) \end{bmatrix} + 1 \right) \right). \end{aligned}$$

In this expression, \hat{q}_{jj} denotes $E[q_{jj}|I_t]$.

2. If $S_t = i$, we use the result from step 1 to solve for PD for the remaining values of κ_t and the same $\{\lambda_{j,t}, \tau_{j,t}\}$.

$$\begin{aligned} & \begin{bmatrix} PD(\kappa_t = 2i - 1, \lambda_{j,t}, \tau_{j,t}) \\ PD(\kappa_t = 2i, \lambda_{j,t}, \tau_{j,t}) \end{bmatrix} = \beta^\alpha \Pi_{B,t,ii,[2i-1:2i]}^T \\ & \times \left(e^{(\rho-\gamma)\tilde{\mu}' + \frac{1}{2}(\rho-\gamma)^2(\tilde{\sigma}')^2 + (1-\rho)\bar{\mu}(q_{ii}, \hat{q}_{jj})} \right. \\ & \left. \circ ((\mathbf{PC}' + 1) \oslash \mathbf{PC})^{\circ(\alpha-1)} \circ (\mathbf{PD}' + 1) \right). \end{aligned}$$

where \mathbf{PD}' is formed by stacking

$$\begin{bmatrix} PD(\kappa_t = 2i - 1, \lambda_{j,t}, \tau_{j,t}) \\ PD(\kappa_t = 2i, \lambda_{j,t}, \tau_{j,t}) \end{bmatrix}, \quad \begin{bmatrix} PC(\kappa_t = 2j - 1, \lambda_{j,t}, \tau_{j,t}) \\ PC(\kappa_t = 2j, \lambda_{j,t}, \tau_{j,t}) \end{bmatrix}$$

appropriately given the values of i and j .

F.5 Both $\{q_{11}, q_{22}\}$ unknown

Using the solutions for both the cases of a single known transition probability, we can now obtain the solution for the case where both transition probabilities are unknown. The transition matrix is now the one given in (A-54). We solve for the equilibrium wealth-consumption and price-dividend ratios on a 5-dimensional grid of values for

$\{\kappa, \lambda_1, \tau_1, \lambda_2, \tau_2\}$ where τ_1 and τ_2 are both truncated at large values $\tau_{1,T}$ and $\tau_{2,T}$, respectively.

F.5.1 Wealth-consumption ratio

We start with the following two approximations:

$$\begin{aligned} PC(\kappa_T, X_T, \theta) &= PC(\kappa_T, \lambda_{2,t}, \tau_{2,t}, q_{11}, \theta) \text{ for some large } \tau_{1,T} \text{ and all } (\lambda_{2,t}, \tau_{2,t}), \\ PC(\kappa_T, X_T, \theta) &= PC(\kappa_T, \lambda_{1,t}, \tau_{1,t}, q_{22}, \theta) \text{ for some large } \tau_{2,T} \text{ and all } (\lambda_{1,t}, \tau_{1,t}). \end{aligned}$$

From here, we iterate back in both the τ_1 and τ_2 dimensions alternately as follows:

1. If $S_t = 1$, $\lambda_{1,t+1}$ and $\tau_{1,t+1}$ will update as above for both $S_{t+1} = 1$ and $S_{t+1} = 2$. This allows us to iterate back one step for τ_1 :

$$\begin{aligned} & \begin{bmatrix} PC(\kappa_t = 1, \lambda_{1,t}, \tau_{1,t}, \lambda_{2,t}, \tau_{2,t})^\alpha \\ PC(\kappa_t = 2, \lambda_{1,t}, \tau_{1,t}, \lambda_{2,t}, \tau_{2,t})^\alpha \end{bmatrix} \\ &= \beta^\alpha \Pi_{B,t,ii,[1:2]}^T \times \left(e^{(1-\gamma)\tilde{\mu}' + \frac{1}{2}(1-\gamma)^2(\tilde{\sigma}')^2} \right. \\ & \quad \times \circ \left(\begin{bmatrix} PC(\kappa_t = 1, \lambda_{1,t+1}, \tau_{1,t} + 1, \lambda_{2,t}, \tau_{2,t}) \\ PC(\kappa_t = 2, \lambda_{1,t+1}, \tau_{1,t} + 1, \lambda_{2,t}, \tau_{2,t}) \\ PC(\kappa_t = 3, \lambda_{1,t+1}, \tau_{1,t} + 1, \lambda_{2,t}, \tau_{2,t}) \\ PC(\kappa_t = 4, \lambda_{1,t+1}, \tau_{1,t} + 1, \lambda_{2,t}, \tau_{2,t}) \end{bmatrix} + 1 \right)^{\circ\alpha} \left. \right). \end{aligned}$$

2. If $S_t = 2$, we analogously iterate back one step for τ_2 :

$$\begin{aligned} & \begin{bmatrix} PC(\kappa_t = 3, \lambda_{1,t}, \tau_{1,t}, \lambda_{2,t}, \tau_{2,t})^\alpha \\ PC(\kappa_t = 4, \lambda_{1,t}, \tau_{1,t}, \lambda_{2,t}, \tau_{2,t})^\alpha \end{bmatrix} \\ &= \beta^\alpha \Pi_{B,t,ii,[3:4]}^T \times \left(e^{(1-\gamma)\tilde{\mu}' + \frac{1}{2}(1-\gamma)^2(\tilde{\sigma}')^2} \right. \\ & \quad \times \circ \left(\begin{bmatrix} PC(\kappa_t = 1, \lambda_{1,t}, \tau_{1,t}, \lambda_{2,t+1}, \tau_{2,t} + 1) \\ PC(\kappa_t = 2, \lambda_{1,t}, \tau_{1,t}, \lambda_{2,t+1}, \tau_{2,t} + 1) \\ PC(\kappa_t = 3, \lambda_{1,t}, \tau_{1,t}, \lambda_{2,t+1}, \tau_{2,t} + 1) \\ PC(\kappa_t = 4, \lambda_{1,t}, \tau_{1,t}, \lambda_{2,t+1}, \tau_{2,t} + 1) \end{bmatrix} + 1 \right)^{\circ\alpha} \left. \right). \end{aligned}$$

F.5.2 Price-dividend ratio

The price-dividend ratio solution is obtained analogously again starting with the following two approximations:

$$\begin{aligned} PD(\kappa_T, X_T, \theta) &= PD(\kappa_T, \lambda_{2,t}, \tau_{2,t}, q_{11}, \theta) \text{ for some large } \tau_{1,T} \text{ and all } (\lambda_{2,t}, \tau_{2,t}), \\ PD(\kappa_T, X_T, \theta) &= PD(\kappa_T, \lambda_{1,t}, \tau_{1,t}, q_{22}, \theta) \text{ for some large } \tau_{2,T} \text{ and all } (\lambda_{1,t}, \tau_{1,t}). \end{aligned}$$

From here, we iterate back in both the τ_1 and τ_2 dimensions alternately as follows:

1. If $S_t = 1$, we iterate back one step for τ_1 :

$$\begin{aligned} &\begin{bmatrix} PD(\kappa_t = 1, \lambda_{1,t}, \tau_{1,t}, \lambda_{2,t}, \tau_{2,t}) \\ PD(\kappa_t = 2, \lambda_{1,t}, \tau_{1,t}, \lambda_{2,t}, \tau_{2,t}) \end{bmatrix} \\ &= \beta^\alpha \Pi_{B,t,ii,[1:2]}^T \times \left(e^{(\rho-\gamma)\tilde{\mu}' + \frac{1}{2}(\rho-\gamma)^2(\tilde{\sigma}')^2 + (1-\rho)\tilde{\mu}(q_{ii}, \hat{q}_{jj})} \circ ((\mathbf{PC}' + 1) \oslash \mathbf{PC})^{\circ(\alpha-1)} \right. \\ &\quad \left. \times \circ \left(\begin{bmatrix} PD(\kappa_t = 1, \lambda_{1,t+1}, \tau_{1,t} + 1, \lambda_{2,t}, \tau_{2,t}) \\ PD(\kappa_t = 2, \lambda_{1,t+1}, \tau_{1,t} + 1, \lambda_{2,t}, \tau_{2,t}) \\ PD(\kappa_t = 3, \lambda_{1,t+1}, \tau_{1,t} + 1, \lambda_{2,t}, \tau_{2,t}) \\ PD(\kappa_t = 4, \lambda_{1,t+1}, \tau_{1,t} + 1, \lambda_{2,t}, \tau_{2,t}) \end{bmatrix} + 1 \right) \right). \end{aligned}$$

2. If $S_t = 2$, we iterate back one step for τ_2 :

$$\begin{aligned} &\begin{bmatrix} PD(\kappa_t = 3, \lambda_{1,t}, \tau_{1,t}, \lambda_{2,t}, \tau_{2,t}) \\ PD(\kappa_t = 4, \lambda_{1,t}, \tau_{1,t}, \lambda_{2,t}, \tau_{2,t}) \end{bmatrix} \\ &= \beta^\alpha \Pi_{B,t,ii,[3:4]}^T \times \left(e^{(\rho-\gamma)\tilde{\mu}' + \frac{1}{2}(\rho-\gamma)^2(\tilde{\sigma}')^2 + (1-\rho)\tilde{\mu}(q_{ii}, \hat{q}_{jj})} \circ ((\mathbf{PC}' + 1) \oslash \mathbf{PC})^{\circ(\alpha-1)} \right. \\ &\quad \left. \times \circ \left(\begin{bmatrix} PD(\kappa_t = 1, \lambda_{1,t}, \tau_{1,t}, \lambda_{2,t+1}, \tau_{2,t} + 1) \\ PD(\kappa_t = 2, \lambda_{1,t}, \tau_{1,t}, \lambda_{2,t+1}, \tau_{2,t} + 1) \\ PD(\kappa_t = 3, \lambda_{1,t}, \tau_{1,t}, \lambda_{2,t+1}, \tau_{2,t} + 1) \\ PD(\kappa_t = 4, \lambda_{1,t}, \tau_{1,t}, \lambda_{2,t+1}, \tau_{2,t} + 1) \end{bmatrix} + 1 \right) \right). \end{aligned}$$

F.6 Asset pricing moments

Using our 5-dimensional solutions for PC and PD , we can obtain analogous solution arrays for the risk-free rate and ex-ante equity risk premium on the same grid of $\{\kappa, \lambda_1, \tau_1, \lambda_2, \tau_2\}$ values using the following equations.

- Risk-free rate:

The risk-free rate in the model is

$$\begin{aligned} \frac{1}{1 + R_t^f} &= E_t [M_{t+1}] \\ &= \beta^\theta E_t \left[e^{-\gamma \tilde{\mu}_{\kappa_{t+1}} + \frac{1}{2} \gamma^2 \tilde{\sigma}_{\kappa_{t+1}}^2} \left(\frac{PC_{t+1} + 1}{PC_t} \right)^{\theta-1} \right]. \end{aligned}$$

Therefore, the log risk-free rate can be approximated by:

$$rf_t \approx \ln(1 + R_t^f) = -\ln \left(\beta^\theta E_t \left[\exp \left\{ -\gamma \tilde{\mu}_{\kappa_{t+1}} + \frac{1}{2} \gamma^2 \tilde{\sigma}_{\kappa_{t+1}}^2 \right\} \left(\frac{PC_{t+1} + 1}{PC_t} \right)^{\theta-1} \right] \right)$$

- Risk premium on equity:

The expected return on equity is:

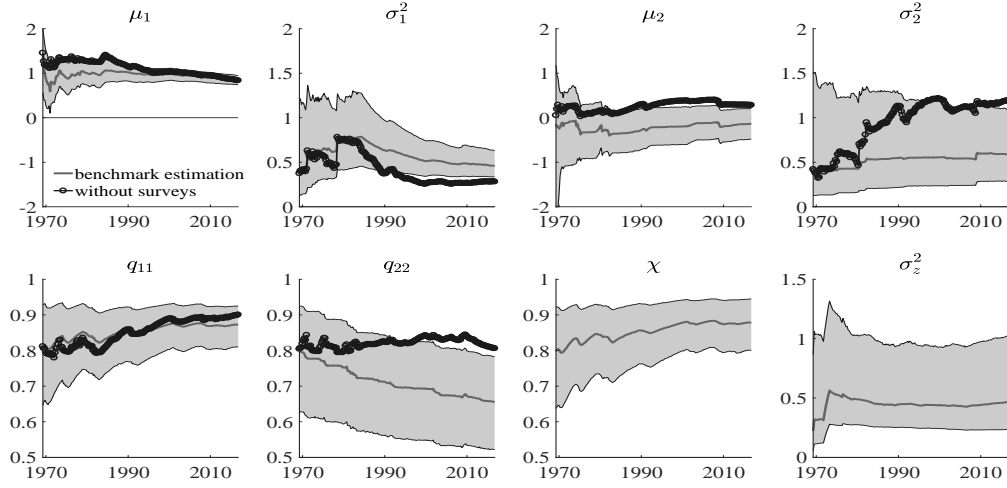
$$\begin{aligned} E_t [1 + R_{e,t+1}] &= E_t \left[\frac{PD_{t+1} + 1}{PD_t} \frac{D_{t+1}}{D_t} \right] \\ &= E_t \left[e^{(1-\rho)\bar{\mu}_{t+1} + \rho \tilde{\mu}_{\kappa_{t+1}} + \frac{1}{2} \rho^2 \tilde{\sigma}_{\kappa_{t+1}}^2 + \frac{1}{2} \sigma_d^2} \frac{PD_{t+1} + 1}{PD_t} \right] \end{aligned}$$

where $\bar{\mu}$ varies over time as beliefs about $\{q_{11}, q_{22}\}$ evolve. Therefore, the log ex-ante expected excess return on equity (adjusted by the Jensen's inequality term) is:

$$\begin{aligned} &\ln \left(\frac{E_t [1 + R_{e,t+1}]}{1 + R_t^f} \right) - \frac{1}{2} \sigma_d^2 \\ &= \ln \left(E_t \left[\exp \left\{ (1-\rho) \bar{\mu}_{t+1} + \rho \tilde{\mu}_{\kappa_{t+1}} + \frac{1}{2} \rho^2 \tilde{\sigma}_{\kappa_{t+1}}^2 \right\} \frac{PD_{t+1} + 1}{PD_t} \right] \right) - rf_t \end{aligned}$$

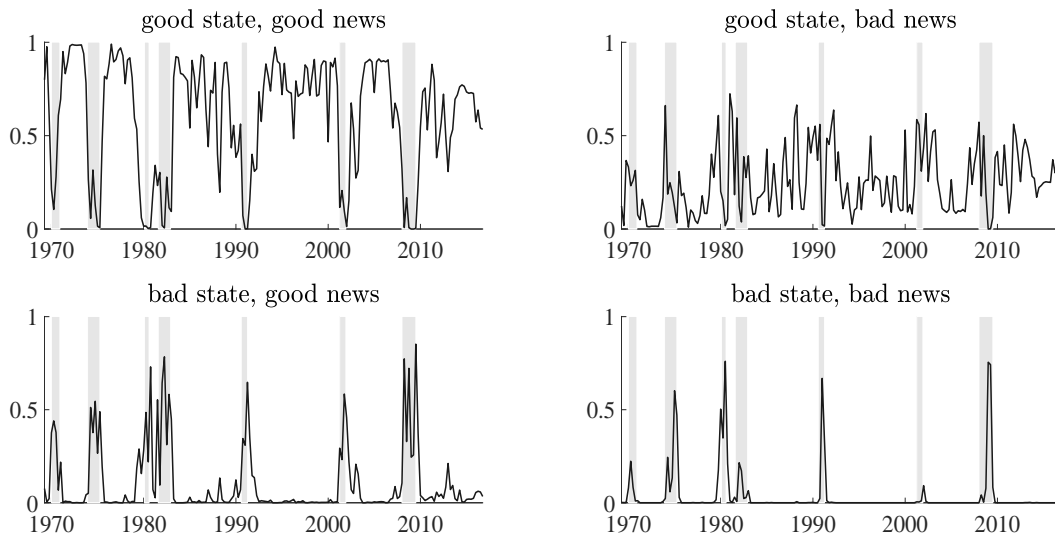
G Supplementary Figures

Figure A-1: Filtered estimates: Parameters



Notes: Gray solid lines are posterior median values which are overlaid with the 90% credible interval (gray shaded areas). Black circled-lines are posterior median values obtained without survey forecasts. To deal with label switching problem, we impose that $\mu_1 > \mu_2$.

Figure A-2: Probability of each regime



Notes: Black solid lines are posterior median values.